Article

Synthesis and Reactivity of Low-Coordinate Iron(II) Fluoride Complexes and Their Use in the Catalytic Hydrodefluorination of Fluorocarbons

Javier Vela, Jeremy M. Smith, Ying Yu, Nicole A. Ketterer, Christine J. Flaschenriem, Rene J. Lachicotte, and Patrick L. Holland

J. Am. Chem. Soc., **2005**, 127 (21), 7857-7870• DOI: 10.1021/ja042672l • Publication Date (Web): 05 May 2005

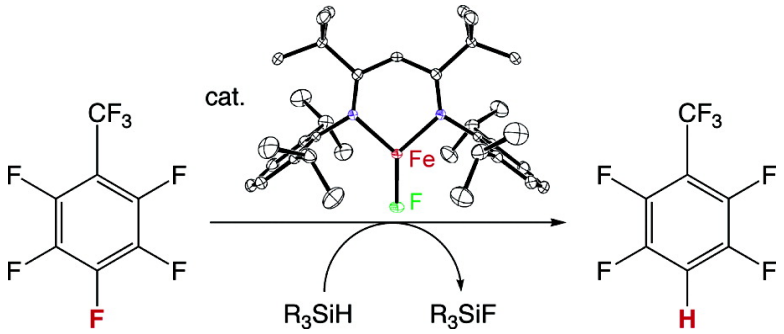

More About This Article

Additional resources and features associated with this article are available within the HTML version:

- Supporting Information
- Links to the 22 articles that cite this article, as of the time of this article download
- Access to high resolution figures
- Links to articles and content related to this article
- Copyright permission to reproduce figures and/or text from this article

View the Full Text HTML

J|A|C|S
ARTICLES
Published on Web 05/05/2005

Synthesis and Reactivity of Low-Coordinate Iron(II) Fluoride Complexes and Their Use in the Catalytic Hydrodefluorination of Fluorocarbons

Javier Vela,[†] Jeremy M. Smith,[†,‡] Ying Yu,[†] Nicole A. Ketterer,[†] Christine J. Flaschenriem,[†] Rene J. Lachicotte,[†] and Patrick L. Holland*[,†]

Contribution from the Department of Chemistry, University of Rochester, Rochester, New York 14627

Received December 6, 2004; E-mail: holland@chem.rochester.edu

Abstract: Transition metal fluoride complexes are of interest because they are potentially useful in a multitude of catalytic applications, including C−F bond activation and fluorocarbon functionalization. We report the first crystallographically characterized examples of molecular iron(II) fluorides: $[L^{Me}Fe(\mu\text{-}F)]_2$ (**1_2**) and $L^{tBu}FeF$ (**2**) (L = bulky β-diketiminate). These complexes react with donor molecules (L′), yielding trigonal-pyramidal complexes $L^RFeF(L')$. The fluoride ligand is activated by the Lewis acid $Et_2O{\cdot}BF_3$, forming $L^{tBu}Fe(OEt_2)(\eta^1\text{-}BF_4)$ (**3**), and is also silaphilic, reacting with silyl compounds such as $Me_3SiSSiMe_3$, $Me_3SiCCSiMe_3$, and Et_3SiH to give new thiolate $L^{tBu}FeSSiMe_3$ (**4**), acetylide $L^{tBu}FeCCSiMe_3$ (**5**), and hydride $[L^{Me}Fe(\mu\text{-}H)]_2$ (**6_2**) complexes. The hydrodefluorination (HDF) of perfluorinated aromatic compounds (hexafluorobenzene, pentafluoropyridine, and octafluorotoluene) with a silane R_3SiH ($R_3 = (EtO)_3$, Et_3, Ph_3, $(3,5\text{-}(CF_3)_2C_6H_3)Me_2$) is catalyzed by addition of an iron(II) fluoride complex, giving mainly the singly hydrodefluorinated products (pentafluorobenzene, 2,3,5,6-tetrafluoropyridine, and α,α,α,2,3,5,6-heptafluorotoluene, respectively) in up to five turnovers. These catalytic perfluoroarene HDF reactions proceed with activation of the C−F bond *para* to the most electron-withdrawing group and are dependent on the degree of fluorination and solvent polarity. Kinetic studies suggest that hydride generation is the rate-limiting step in the HDF of octafluorotoluene, but the active intermediate is unknown. Mechanistic considerations argue against oxidative addition and outer-sphere electron transfer pathways for perfluoroarene HDF. Fluorinated olefins are also hydrodefluorinated (up to 10 turnovers for hexafluoropropene), most likely through a hydride insertion/β-fluoride elimination mechanism. Complexes **1_2** and **2** thus provide a rare example of a homogeneous system that activates C−F bonds without competitive C−H activation and use an inexpensive 3d transition metal.

Introduction

Fluorine's peculiar characteristics such as high electronegativity, low polarizability, and small covalent radius render fluorocarbons thermally stable, water repellent, and resistant to chemical degradation.[1] These unique properties, along with the great strength of the C−F bond (120−129 kcal/mol for aliphatic and olefinic C−F bonds, and up to 154 kcal/mol in C_6F_6),[2] make fluorocarbons valuable refrigerants, pesticides, and nonadhesive polymers but also very environmentally persistent. Therefore, methods for chemically manipulating fluorocarbons are sought to either degrade or add value to these materials.

Great advances have been made in recent years on the intra-[3] and intermolecular activation of aromatic,[4] olefinic,[5] and even aliphatic[6] fluorocarbons by homogeneous transition metal complexes.[7] Metal fluoride complexes[8−10] are often formed during these C−F activation reactions, and they can potentially be recycled to make these reactions catalytic. Scheme 1 shows a few examples of well-studied C−F activation reactions. Often, an early transition metal drives the reaction through formation of a very strong M−F bond, but the resultant compound is inert (for example Cp^*_2ZrHF).[7a] To catalytically functionalize C−F

[†] University of Rochester.
[‡] Current address: Department of Chemistry & Biochemistry, New Mexico State University, Las Cruces, NM 88003.

(1) (a) Lemal, D. M. *J. Org. Chem.* **2004**, 69, 1−11. (b) Sanford, G. *Tetrahedron* **2003**, 59, 437−454. (c) Hiyama, T. *Organofluorine Compounds: Chemistry and Applications*; Springer: Berlin, 2000.

(2) (a) Kerr, J. A. In *CRC Handbook of Chemistry and Physics*, 71st ed.; Lide, R. L., Ed.; CRC Press: Boca Raton, FL, 1990; pp 9.65−9.98. (b) Smart, B. E. *Mol. Struct. Energ.* **1986**, *3*, 141−191. (c) Smart, B. E. In *The Chemistry of Functional Groups, Supplement D*; Pati, S., Rappoport, Z., Eds.; John Wiley & Sons: New York, 1983; Chapter 14.

(3) Representative examples of intramolecular C−F activation: (a) Richmond, T. G. *Angew. Chem., Int. Ed.* **2000**, *39*, 3241−3244. (b) Hughes, R. P.; Zhang, D.; Zakharov, L. N.; Rheingold, A. L. *Organometallics* **2002**, *21*, 4902−4904. (c) Hughes, R. P.; Laritchev, R. B.; Zakharov, L. N.; Rheingold, A. L. *J. Am. Chem. Soc.* **2004**, *126*, 2308−2309. (d) Hughes, R. P.; Lindner, D. C.; Rheingold, A. L.; Liable-Sands, L. M. *J. Am. Chem. Soc.* **1997**, *119*, 11544−11545. (e) Hughes, R. P.; Smith, J. M. *J. Am. Chem. Soc.* **1999**, *121*, 6084−6085. (f) Albietz, P. J.; Houlis, J. F.; Eisenberg, R. *Inorg. Chem.* **2002**, *41*, 2001−2003.

(4) Representative examples of intermolecular aromatic C−F activation: (a) Jasim, N. A.; Perutz, R. N.; Whitwood, A. C.; Braun, T.; Izundu, J.; Neumann, B.; Rothfeld, S.; Stammler, H.-G. *Organometallics* **2004**, *23*, 6140−6149. (b) Edelbach, B. L.; Jones, W. D. *J. Am. Chem. Soc.* **1997**, *119*, 7734−7742. (c) Cronin, L.; Higgitt, C. L.; Karch, R.; Perutz, R. N. *Organometallics* **1997**, *16*, 4920−4928. (d) Harrison, R. G.; Richmond, T. G. *J. Am. Chem. Soc.* **1993**, *115*, 5303−5304. (e) Bennett, B. K.; Harrison, R. G.; Richmond, T. G. *J. Am. Chem. Soc.* **1994**, *116*, 11165−11166. (f) Whittlesey, M. K.; Perutz, R. N.; Moore, M. H. *Chem. Commun.* **1996**, 787−788.

Scheme 1

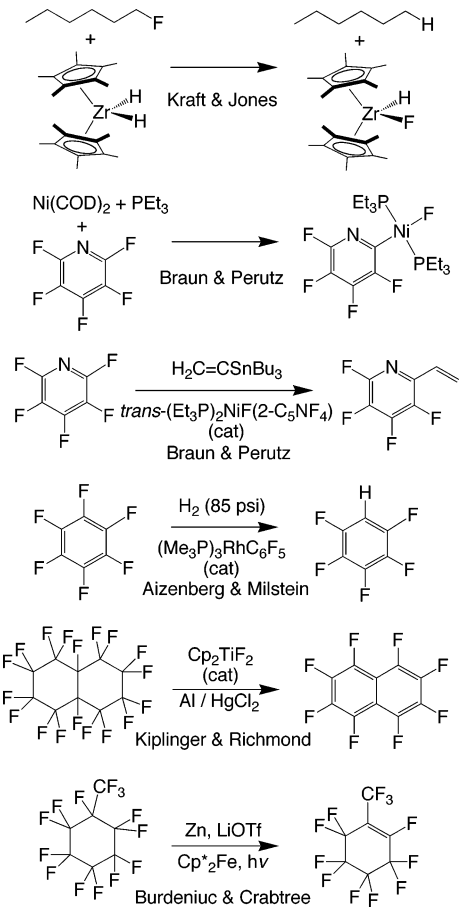

bonds,[11−14] late transition metals may be more suitable because their M−F bonds are not prohibitively strong and also because late metals are more tolerant of functional groups. The work of Milstein in particular has shown the effectiveness of rhodium compounds in the catalytic hydrodefluorination (HDF) of aromatic perfluorocarbons.[12a,b] However, the examples of catalytic C−F activation by homogeneous metal complexes are few, and research is needed to progress toward applications.

As part of our research program on low-coordinate late metal chemistry,[15−17] we were attracted to low-coordinate iron fluoride complexes, anticipating high reactivity due to the unsaturated metal and the exposed fluoride ligand. We present here the synthesis and characterization of iron(II) fluoride complexes and report that these complexes serve as valuable synthetic precursors as well as precatalysts in the catalytic hydrodefluorination of fluorocarbons.

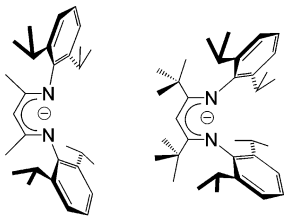

Figure 1. Diketiminate ligands used in this work.

Results and Discussion

Synthesis and Behavior of Diketiminate Iron(II) Fluorides. We previously have reported three-coordinate iron(II) hydrocarbyl complexes based on the diketiminate ligands L^{Me} and L^{tBu} (Figure 1).[18] These complexes serve as precursors to discrete iron(II) fluorides by reaction with trimethyltin fluoride (Scheme 2).[19] Because Me_3SnF is poorly soluble in toluene, alkyl complexes of L^{Me} are treated with an excess of the insoluble fluorinating agent, and unreacted Me_3SnF is removed from the reaction mixture by filtration. In a typical reaction, $[L^{Me}FeF]_2$ (**1$_2$**) is isolated in 83% yield as a bright green powder that readily dissolves in hydrocarbon solvents such as diethyl ether, toluene, or THF. Its dimeric nature is shown in the X-ray crystal structure (Figure 2).

(5) Representative examples of olefinic C−F activation: (a) Braun, T.; Noveski, D.; Neumann, B.; Stammler, H.-G. *Angew. Chem., Int. Ed.* **2002**, *42*, 2745−2748. (b) Kraft, B. M.; Jones, W. D. *J. Am. Chem. Soc.* **2002**, *124*, 8681−8689. (c) Kirkham, M. S.; Mahon, M. F.; Whittlesey, M. K. *Chem. Commun.* **2001**, 813−814. (d) Noveski, D.; Braun, T.; Schulte, M.; Neumann, B.; Stammler, H.-G. *Dalton Trans.* **2003**, 4075−4083. (e) Peterson, T. H.; Golden, J. T.; Bergman, R. G. *Organometallics* **1999**, *18*, 2005−2020. (f) Siedle, A. R.; Newark, R. A. *Organometallics* **1989**, *8*, 1442−1450. (g) Watson, L. A.; Yandulov, D. V.; Caulton, K. G. *J. Am. Chem. Soc.* **2001**, *123*, 603−611. (h) Watson, P. L.; Tulip, T. H.; Williams, I. *Organometallics* **1990**, *9*, 1999−2009. (i) Ferrando-Miguel, G.; Gérard, H.; Eisenstein, O.; Caulton, K. G. *Inorg. Chem.* **2002**, *41*, 6440−6449.
(6) Aliphatic C−F activation: (a) Kraft, B. M.; Lachicotte, R. J.; Jones, W. D. *J. Am. Chem. Soc.* **2000**, *122*, 8559−8560. (b) Kraft, B. M.; Lachicotte, R. J.; Jones, W. D. *J. Am. Chem. Soc.* **2001**, *123*, 10973−10979.
(7) (a) Jones, W. D. *Dalton* **2003**, 3991−3995. (b) Braun, T.; Perutz, R. N. *Chem. Commun.* **2002**, 2749−2757. (c) Burdeniuc, J.; Jedlicka, B.; Crabtree, R. H. *Chem. Ber.* **1997**, *130*, 145−154. (d) Kiplinger, J. L.; Richmond, T. G.; Osterberg, C. E. *Chem. Rev.* **1994**, *94*, 373−431. (e) Mazurek, U.; Scwarz, H. *Chem. Commun.* **2003**, 1321−1326. (f) Richmond, T. G. Metal Reagents for Activation and Functionalization of Carbon−Fluorine Bonds. In *Activation of Unreactive Bonds in Organic Synthesis*; Murai, S., Ed.; Springer: Berlin, 1999; pp 243−269.
(8) (a) Pagenkopf, B. L.; Carreira, E. M. *Chem. Eur. J.* **1999**, *5*, 3437−3442. (b) Grushin, V. V. *Chem. Eur. J.* **2002**, *8*, 1007−1014. (c) Verdaguer, X.; Lange, U. E. W.; Reding, M. T.; Buchwald, S. L. *J. Am. Chem. Soc.* **1996**, *118*, 6784−6785.
(9) (a) Grushin, V. V.; Marshall, W. J. *J. Am. Chem. Soc.* **2004**, *126*, 3068−3069. (b) Grushin, V. V. *Angew. Chem., Int. Ed.* **1998**, *37*, 994−996.
(10) (a) Murphy, E. F.; Murugavel, R.; Roesky, H. W. *Chem. Rev.* **1997**, *97*, 3425−3468. (b) Doherty, N. M.; Hoffman, N. W. *Chem. Rev.* **1991**, *91*, 553−573.
(11) Heterogeneous catalytic C−F activation: (a) Burdeniuc, J.; Crabtree, R. H. *Organometallics* **1998**, *17*, 1582−1586. (b) Stanger, K. J.; Angelici, R. J. *J. Mol. Catal. A: Chem.* **2004**, *207*, 59−68. (c) Kiplinger, J. L.; Richmond, T. G. *J. Am. Chem. Soc.* **1996**, *118*, 1805−1806. (d) Yang, H.; Gao, H.; Angelici, R. J. *Organometallics* **1999**, *18*, 2285−2287. (e) Young, R. J.; Grushin, V. V. *Organometallics* **1999**, *18*, 284−296.
(12) Homogeneous catalytic C−F activation with transition metal complexes: (a) Aizenberg, M.; Milstein, D. *Science* **1994**, *265*, 359−361. (b) Aizenberg, M.; Milstein, D. *J. Am. Chem. Soc.* **1995**, *117*, 8674−8675. (c) Ishii, Y.; Chatani, N.; Yorimitsu, S.; Murai, S. *Chem. Lett.* **1998**, 157−158. (d) Braun, T.; Perutz, R. N.; Sladek, M. I. *Chem. Commun.* **2001**, 2254−2255. (e) Kuhl, S.; Schneider, R.; Fort, Y. *Adv. Synth. Catal.* **2003**, *345*, 341−344.
(13) Silyl cations can mediate catalytic C−F activation: (e) Scott, V. J.; Çelenligil-Çetin, R.; Ozerov, O. V. *J. Am. Chem. Soc.* **2005**, *127*, 2852−2853.
(14) Catalytic C−F activation through cross-metathesis reactions: (a) Widdowson, D. A.; Wilhelm, R. *Chem. Commun.* **1999**, 2211−2212. (b) Böhm, V. P. W.; Gstöttmayr, C. W. K.; Weskamp, T.; Herrmann, W. A. *Angew. Chem., Int. Ed.* **2001**, *40*, 3387−3389.
(15) (a) Eckert, N. A.; Smith, J. M.; Lachicotte, R. J.; Holland, P. L. *Inorg. Chem.* **2004**, *43*, 3306−3321. (b) Eckert, N. A.; Bones, E. M.; Lachicotte, R. J.; Holland, P. L. *Inorg. Chem.* **2003**, *42*, 1720−1725. (c) Holland, P. L.; Cundari, T. R.; Perez, L. L.; Eckert, N. A. E.; Lachicotte, R. J. *J. Am. Chem. Soc.* **2002**, *124*, 14416−14424. (d) Andres, H.; Bominaar, E. M.; Smith, J. M.; Eckert, N. A. E.; Holland, P. L.; Münck, E. *J. Am. Chem. Soc.* **2002**, *124*, 3012−3025. (e) Smith, J. M.; Lachicotte, R. J.; Pittard, K. A.; Cundari, T. R.; Lukat-Rodgers, G.; Rodgers, K. R.; Holland, P. L. *J. Am. Chem. Soc.* **2001**, *123*, 9222−9223. (f) Smith, J. M.; Lachicotte, R. J.; Holland, P. L. *Chem Commun.* **2001**, 1342−1343.
(16) Vela, J.; Stoian, S.; Flaschenriem, C. J.; Münck, E.; Holland, P. L. *J. Am. Chem. Soc.* **2004**, *126*, 4522−4523.
(17) Smith, J. M.; Lachicotte, R. J.; Holland, P. L. *J. Am. Chem. Soc.* **2003**, *125*, 15752−15753.
(18) (a) Vela, J.; Vaddadi, S.; Cundari, T. R.; Smith, J. M.; Gregory, E. A.; Lachicotte, R. J.; Flaschenriem, C. J.; Holland, P. L. *Organometallics* **2004**, *23*, 5226−5239. (b) Vela, J.; Smith, J. M.; Lachicotte, R. J.; Holland, P. L. *Chem. Commun.* **2002**, 2886−2887. (c) Smith, J. M.; Lachicotte, R. J.; Holland, P. L. *Organometallics* **2002**, *21*, 4808−4814.
(19) Krause, E. *Ber. Dtsch. Chem. Ges.* **1918**, 1447.

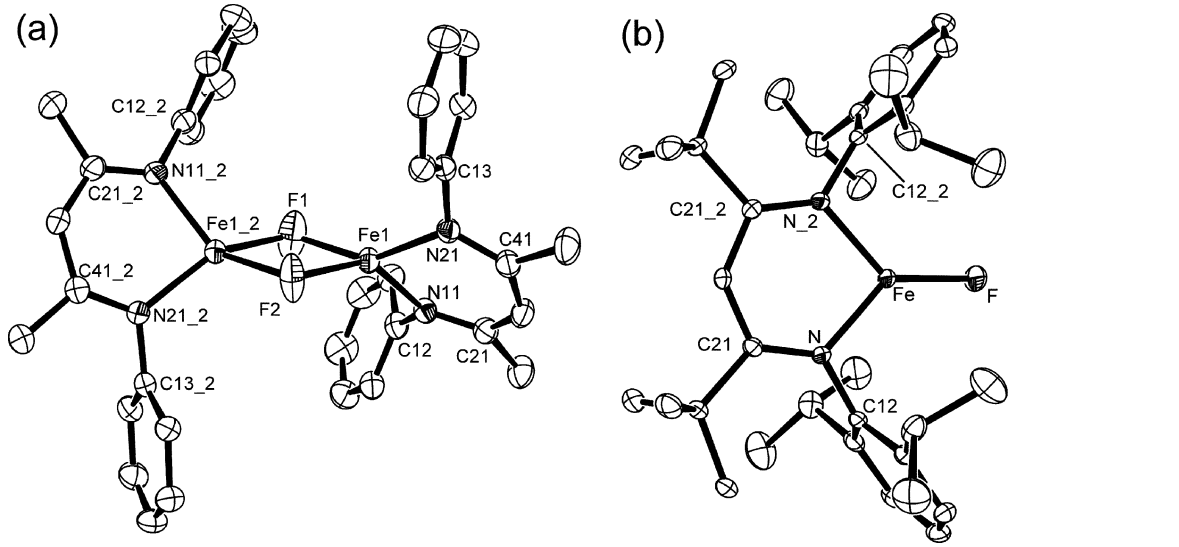

Figure 2. Molecular structures of $\mathbf{1_2}$ (a) and **2** (b). Ellipsoids are shown at 50% probability. Hydrogen atoms, and isopropyl groups in $\mathbf{1_2}$, are omitted for clarity.

Scheme 2

$$L^{R}FeR' + Me_3SnF \longrightarrow [L^{R}FeF]_n + Me_3SnR'$$

$$n = 2(L^{Me}),\ 1(L^{tBu});\ R' = Me,\ {}^{n}Pr,\ {}^{i}Bu,\ Cy$$

When Me_3SnF is reacted with an alkyl complex of the more sterically demanding ligand L^{tBu} (Figure 1), the pink iron product shows low solubility in pentane, toluene, and diethyl ether. Therefore, in this case, a slight excess of the highly soluble alkyliron(II) complex is used, and pentane is used to wash out the remaining alkyl complex. This leads to a 74% yield of $L^{tBu}FeF$ (**2**), which was also characterized by X-ray diffraction (Figure 2, discussed below). The low solubility of **2** is attributable to the high dipole moment along the Fe−F bond caused by the electronegative fluorine, as well as to exposure of the hard fluoride ligand to the molecule's surface. As a result, **2** dissolves only in coordinating solvents such as THF and acetonitrile (see below for details). In contrast, the complex $[L^{Me}FeF]_2$ ($\mathbf{1_2}$) is very soluble in hydrocarbons because the molecule has a low dipole moment and the fluoride ligands are buried within the hydrocarbon ligand framework.

These synthetic routes seem to be general in scope because different alkyliron(II) compounds (methyl, isobutyl, and cyclohexyl)[18] give the iron(II) fluorides in similar yields. Noteworthy is the use of Me_3SnF to prepare iron(II) fluorides since this tin reagent has mainly been used for making early and main group but not late-metal fluoride complexes.[10a,20]

Characterization of Iron(II) Fluoride Complexes. Both $\mathbf{1_2}$ and **2** are paramagnetic at room temperature. For $\mathbf{1_2}$ the solution magnetic moment is 6.2(3) μ_B (per dimer), whereas for **2** the magnetic moment is 5.6(3) μ_B. The paramagnetism is evident in their ^{1}H NMR spectra, which have highly shifted resonances reminiscent of those from other iron(II) diketiminate complexes. The assignments for the ^{1}H NMR resonances are based on relative integrations, similar to the previously characterized diketiminate-iron(II) complexes,[15] and are given in detail in the Experimental Section. Neither $\mathbf{1_2}$ or **2** shows ^{19}F resonances between 500 and −500 ppm (vs $CFCl_3$, THF-d_8), presumably because of very rapid relaxation of the ^{19}F nuclei.

No discrete iron(II) fluoride has previously been structurally characterized.[10,21−23] The molecular iron(II) fluoride Cp*(dppe)Fe^{II}F (an 18-electron complex) was recently synthesized from $[Cp^*(dppe)Fe^{II}]^+PF_6^-$ and CsF or $CoCp_2$.[21] This fluoride complex was too unstable for X-ray diffraction analysis, although a DFT-optimized structure yielded a theoretical Fe−F distance of 1.927 Å. A tris(pyrazolyl)borate iron(II) fluoride has also been isolated.[23]

Table 1. Selected Interatomic Distances (Å) and Angles (deg) for Diketiminate Iron(II) Fluoride Complexes

	$[L^{Me}Fe(\mu\text{-}F)]_2$ ($\mathbf{1_2}$)	$L^{tBu}FeF$ (**2**)
Fe−F	1.9757(12), 1.9774(14)	1.8079(15)
Fe−N	2.0081(18), 2.0161(17)	1.9609(14)
C−N−C	119.92(18), 117.32(18)	127.95(13)
N−Fe−N	93.27(7)	95.66(8)
Fe···Fe	3.0831(6)	
Fe−F−Fe	102.44(10), 102.56(9)	

$L^{tBu}FeF$ (**2**, formally a 12-electron complex) is to our knowledge the *only three-coordinate fluoride complex of any transition metal*. In **2**, iron lies in a crystallographically required planar geometry. Experimental distances for transition metal−fluorine bonds average 1.91 Å (standard deviation 0.09 Å), and thus the Fe−F distance in $L^{tBu}FeF$ (**2**), 1.8079(15) Å, is exceptionally short. Likely reasons for the short Fe−F bond length include the low coordination number at iron and the fluoride's ability to act as a π-donor toward the unsaturated metal.[24] This small terminal Fe−F distance is consistent with the short Fe^{II}−OR bond distances observed in other three-coordinate iron(II) complexes (examples: $L^{R}FeO^{t}Bu$ 1.761(10) Å (R = Me), 1.786(3) Å (R = ^{t}Bu) and $L^{Me}FeOCHPh_2$ 1.8076(16) Å).[15a,18a,25]

The $[Fe(\mu\text{-}F)]_2$ rhomb in $\mathbf{1_2}$ has Fe−F−Fe and F−Fe−F angles of 102.44−102.56° and 77.50(7)°, respectively. The Fe−

(20) (a) Herzog, A.; Roesky, H. W.; Jäger, F.; Steiner, A. *Chem. Commun.* **1996**, 29−30. (b) Herzog, A.; Liu, F.; Roesky, H. W.; Demsar, A.; Keller, K.; Noltemeyer, M.; Pauer, F. *Organometallics* **1994**, *13*, 1251−1256.
(21) Tilset, M.; Fjeldahl, I.; Hamon, J.; Hamon, P.; Toupet, L.; Saillard, J.; Costuas, K.; Haynes, A. *J. Am. Chem. Soc.* **2001**, *123*, 9984−10000.
(22) Cambridge Structural Database, ConQuest version 1.7, November 2004 release. (a) Allen, F. H. *Acta Crystallogr.* **2002**, *B58*, 380−388. (b) Bruno, I. J.; Cole, J. C.; Edgington, P. R.; Kessler, M.; Macrae, C. F.; McCabe, P.; Pearson, J.; Taylor, R. *Acta Crystallogr.* **2002**, *B58*, 389−397.
(23) Gorrell, I. B.; Parkin, G. *Inorg. Chem.* **1990**, *29*, 2452−2456.
(24) (a) Becker, C.; Kieltsch, I.; Broggini, D.; Mezzetti, A. *Inorg. Chem.* **2003**, *42*, 8417−8429. (b) Mezzetti, A.; Becker, C. *Helv. Chim. Acta* **2002**, *85*, 2686−2703. (c) Caulton, K. G. *New J. Chem.* **1994**, *18*, 25−41.

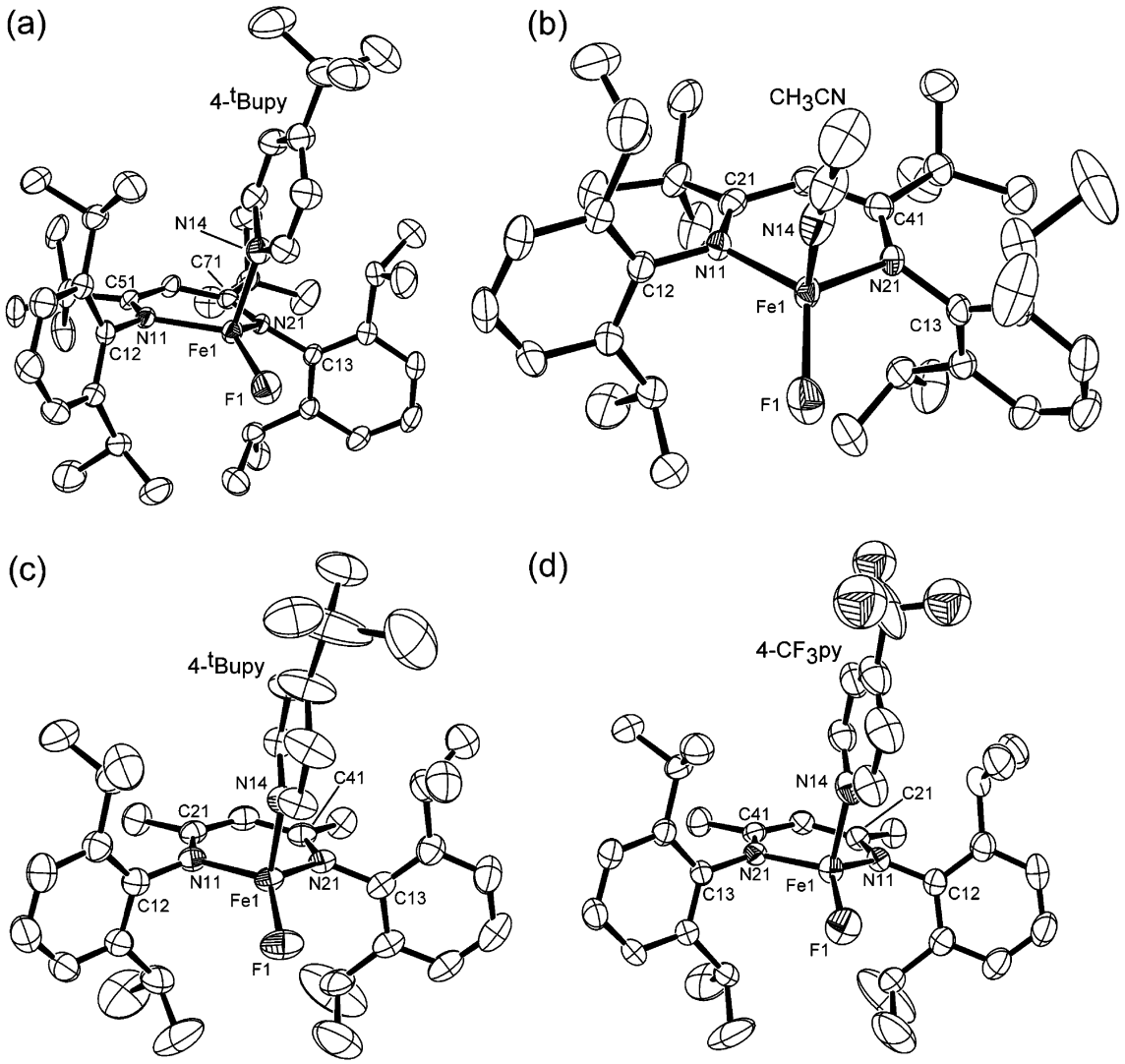

Figure 3. Molecular structures of **2·^{t}Bupy** (a), **2·ACN** (b), **1·^{t}Bupy** (c), and **1·CF$_3$py** (d). Ellipsoids are shown at 50% probability, and hydrogen atoms are omitted for clarity.

(μ-F) distances of about 1.97 Å are between the range of M−(μ-F) distances reported for nickel (1.89−1.91 Å) and manganese (1.95−2.05 Å) complexes with bridging fluoride ligands.[10a] The difference in coordination number and nuclearity between $\mathbf{1_2}$ and **2** has a steric origin. The ligand L^{tBu} is substantially more hindering than L^{Me}: we have previously quantified this steric effect using the C−N−C angle at the imine nitrogen, which is roughly 8° larger in L^{tBu} than L^{Me}.[18a,15f] This trend holds in chloride[15f] and alkyl[18a] complexes of iron(II) bearing the diketiminates L^{Me} and L^{tBu} (Figure 1). Similarly, in the fluoride complexes the C−N−C angle is 127.95° for **2** (L^{tBu}) and 119.92−117.32° for $\mathbf{1_2}$ (L^{Me}) (Table 1).

The infrared (IR) spectrum of **2** (KBr pellet, 450−4000 cm^{-1}) shows a strong band at 596 cm^{-1}. This band lies in the range reported for terminal M−F bond stretching vibrations (ν_{M-F}: 500−750 cm^{-1})[10a,26] and is absent in the IR spectrum of L^{tBu}FeCl[15f] (ν_{M-Cl} range: 200−400 cm^{-1}).[26] Therefore, we assign this band to the iron−fluorine stretching vibration in **2**. For comparison, Perutz and co-workers have reported that the Ni−F stretching vibrations in *trans*-Ni(Et$_3$P)$_2$(C$_6$F$_5$)(F) and *trans*-Ni(Et$_3$P)$_2$(2-C$_5$F$_4$N)(F) appear at 535 and 530 cm^{-1}, respectively, while the chloride complexes *trans*-Ni(Et$_3$P)$_2$-(C$_6$F$_5$)(Cl) and *trans*-Ni(Et$_3$P)$_2$(5-chloro-2,4,6-trifluoro-3-pyridyl)(Cl) do not show any absorptions between 430 and 600 cm^{-1}.[4c] The IR spectrum of the dimeric fluoride complex $\mathbf{1_2}$ (KBr pellet) has no bands between 450 and 1000 cm^{-1} that could be attributed to the Fe−F bond. This is consistent with elongation and overall weakening of the Fe−F bond to bridging fluoride ligands.

The visible spectrum (Figure 4) of the free three-coordinate fluoride **2** has a single absorption maximum at 530 nm (730 M^{-1}cm^{-1}). This band is very similar to that seen in L^{tBu}FeCl, which has λ_{max} = 560 nm (520 M^{-1}cm^{-1}).[15f] We tentatively assign this band to an iron-to-diketiminate (MLCT) transition, reasoning that the more polarized M−F bond leads to a more electrophilic metal and lower d-orbital energies.[27]

Monomeric Four-Coordinate Iron(II) Fluorides. Treatment of the fluoride complex $\mathbf{1_2}$ or **2** with 1 equiv of pyridines or excess acetonitrile is accompanied by a substantial shift in the

(25) (a) Kornev, A. N.; Chesnokova, T. A.; Semenov, V. V.; Zhezlova, E. V.; Zakharov, L. N.; Klapshina, L. G.; Domrachev, G. A.; Rusakov, V. S. *J. Organomet. Chem.* **1997**, *547*, 113−119. (b) Gibson, V. C.; Marshall, E. L.; Navarro-Llobet, D.; White, A. J. P.; Williams, D. J. *J. Chem. Soc., Dalton Trans.* **2002**, 4321−4322. (c) Chen, H.; Power, P. P.; Shoner, S. C. *Inorg. Chem.* **1991**, *30*, 2884−2888. (d) Shannon, R. D. *Acta Crystallogr.* **1976**, *A32*, 751−767.

(26) Nakamoto, K. *Infrared and Raman Spectra of Inorganic Compunds, part B*, 5th ed.; Wiley: New York, 1997; pp 180−190.

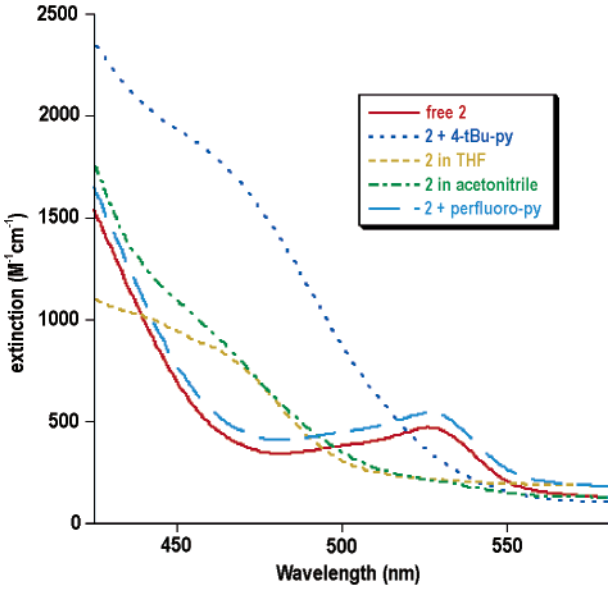

Figure 4. Electronic absorption spectra of three- and four-coordinate iron(II) fluoride complexes of L^{tBu}.

Scheme 3

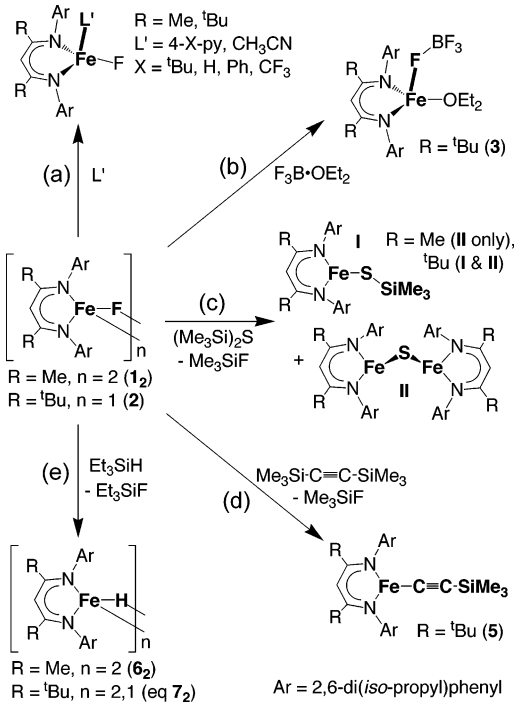

^{1}H NMR resonances as well as a color change (see below), indicative of adduct formation (Scheme 3a). Slow concentration of these solutions leads to crystallization of the four-coordinate complexes L^{tBu}FeF(4-^{t}Bu-py) (**2·^{t}Bupy**), L^{tBu}FeF(NCCH$_3$) (**2·ACN**), L^{Me}FeF(4-^{t}Bu-py) (**1·^{t}Bupy**), and L^{Me}FeF(4-CF$_3$-py) (**1·CF$_3$py**). The molecular structures of these adducts are shown in Figure 3. These complexes are also paramagnetic, having solution magnetic moments of 5.0(4) μ_B, consistent with a high-spin Fe^{II} center.

In the new four-coordinate fluoride complexes, the coordination sphere of iron substantially deviates from a tetrahedral geometry toward a trigonal pyramidal structure, as observed

(27) An alternative assignment is a halide-to-metal LMCT.

Table 2. Structural Parameters of Four-Coordinate Iron(II) Fluoride Complexes

Cmpd(L_{apical})	Fe–F (Å)	Fe–X (Å)	τ^a
L^{tBu}FeF(4-^{t}Bu-py) (**2·^{t}Bupy**)	1.8700(14)	2.1190(19)	0.45
L^{Me}FeF(4-^{t}Bu-py) (**1·^{t}Bupy**)	1.8393(23)	2.1137(30)	0.43
L^{Me}FeF(4-CF$_3$-py) (**1·CF$_3$py**)	1.871(3)	2.115(4)	0.45
L^{tBu}FeF(NCCH$_3$) (**2·ACN**)	1.946(2)	2.099(4)	0.34
L^{tBu}FeOEt$_2$(η^1-BF$_4$) (**3**)	2.0672(10)	2.0404(11)	0.13
[L^{Me}Fe(μ-F)]$_2$ (**1$_2$**)	1.9757(12)	1.9774(14)	0.08

^{a} $\tau = [\Sigma(L_{basal}-Fe-L_{basal}) - \Sigma(L_{basal}-Fe-L_{axial})]/90$. See ref 16.

recently in related sulfido,[16] hydrido,[17] and amido iron(II)[15a] complexes. The extent of this pyramidal distortion can be quantified using τ, which has ideal values of $\tau = 1$ and $\tau = 0$ for perfect trigonal pyramidal (where the metal sits in the plane of the three basal ligands) and tetrahedral geometries, respectively.[16] Table 2 shows the Fe−F distances and τ values for a series of four-coordinate fluoride complexes. We recently have described the tendency for π-donor ligands to prefer the basal position and explained it in terms of a crystal-field model in which the only doubly occupied d orbital has the appropriate symmetry to undergo π-interactions with the axial ligand, but not the basal ligand.[15a] Accordingly, the π-donor fluoride is expected to occupy the basal position, and the π-acceptor pyridines the axial position. This idea is further supported here by the trend in axial distortions: acetonitrile induces a lower distortion from tetrahedral geometry ($\tau = 0.34$)[16] than the stronger π-acceptor pyridines ($\tau = 0.43-0.45$).

The four-coordinate adducts of **2** have a strong band in the IR spectrum attributable to ν_{Fe-F} at 544 cm^{-1} in **2·^{t}Bupy** (Fe−F 1.8700(14) Å) and 538 cm^{-1} in **2·ACN** (Fe−F 1.946(2) Å), lower than that observed for the free three-coordinate fluoride complex (**2**: 596 cm^{-1}, Fe−F 1.8079(15) Å). Interestingly, the fluoride complexes of L^{Me} have a somewhat higher Fe−F stretching frequency: the monomeric adducts of **1** have ν_{Fe-F} at 717 cm^{-1} in **1·^{t}Bupy** (Fe−F 1.8393(23) Å), 704 cm^{-1} in **1·py**, 690 cm^{-1} in **1·Phpy**, and 669 cm^{-1} in **1·CF$_3$py** (Fe−F 1.871(3) Å). These data show that the Fe−F bond elongates and weakens for complexes of a given diketiminate ligand as the σ-donating ability of the pyridine ligand decreases.

In contrast to the three-coordinate fluoride complex **2** (λ_{max} = 530 nm), the visible spectra of the four-coordinate complexes in toluene (including the dimeric fluoride **1$_2$**) show absorption bands near 460 nm (930−2110 M^{-1} cm^{-1}) (Figure 4). Addition of 1 equiv of pentafluoropyridine causes no change in the visible spectrum of **2**, indicating that it does not coordinate. Conversely, tetrahydrofuran and acetonitrile solutions of **2** show the 460 nm maximum indicative of adduct formation (Figure 4). Therefore, we conclude that solubilization of **2** in THF is accompanied by formation of the four-coordinate fluoride L^{tBu}FeF(THF) (similar to the structurally characterized **2·ACN**).

A series of pyridine adducts with the fluoride complex of L^{Me} (**1**·L′) show two absorption bands in the visible spectrum: one very similar to the four-coordinate complexes derived from **2** (λ_{max} = 400−420 nm, 1630−2180 M^{-1}cm^{-1}) and another one that shifts to higher energy when the electron-donating ability of the pyridine (L′) increases (λ_{max} = 512 nm (670 M^{-1} cm^{-1}) for CF$_3$py; λ_{max} = 465 nm (1260 M^{-1} cm^{-1}) for ^{t}Bupy). This latter band may thus be assigned as a MLCT transition between the iron and the pyridine ligand.

All four coordinate fluoride complexes derived from **1$_2$** and **2** also possess an electronic absorption between 900 and 980

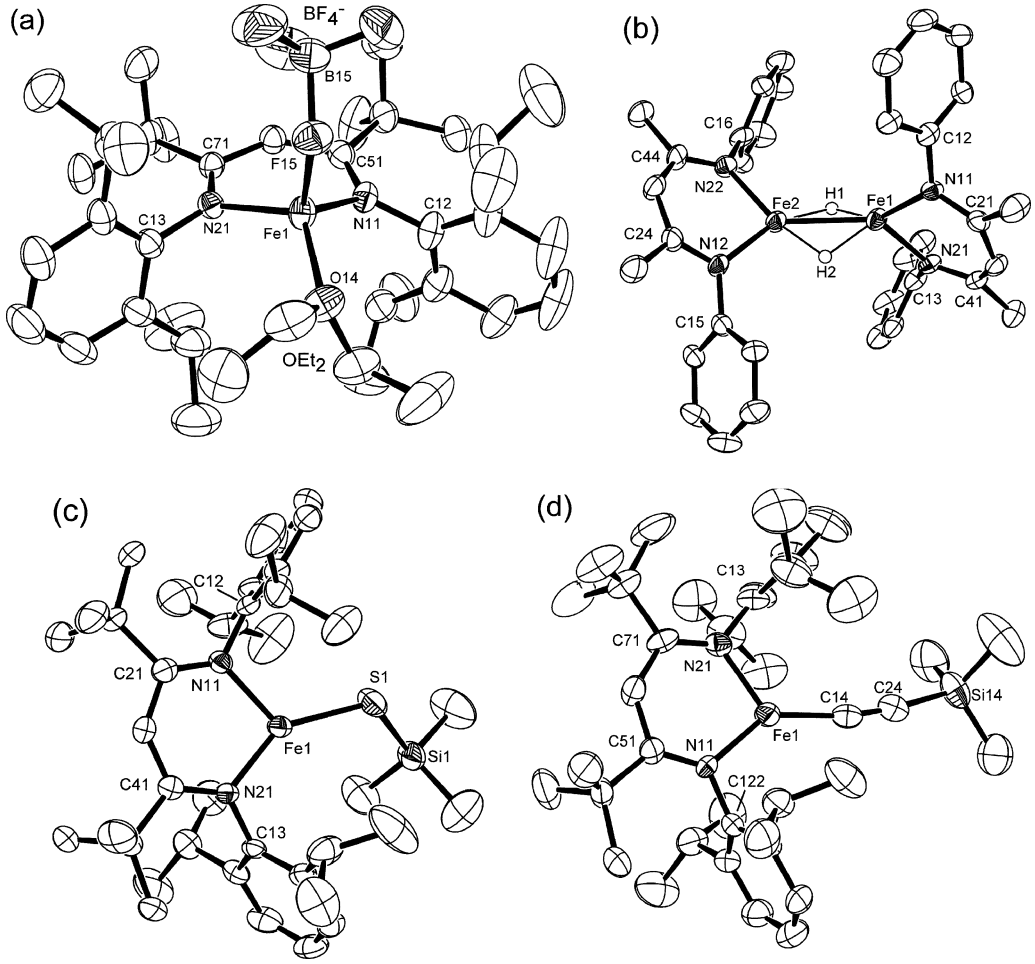

Figure 5. Molecular structures of **3** (a), $\mathbf{6_2}$ (b), **4** (c), and **5** (d). Ellipsoids are shown at 50% probability. Carbon-bound hydrogen atoms, and isopropyl groups in $\mathbf{6_2}$, are omitted for clarity.

nm. A similar band is observed for the parent fluoride complexes $\mathbf{1_2}$ and **2** at 791 and 715 nm, respectively. Because this absorption occurs at a lower energy and has a lower intensity (90−210 M^{-1} cm^{-1}) than the absorptions mentioned above, we assign it as a d−d transition.

Disruption of the Fe−F Bond by Boron and Silicon Reagents. Treatment of a slurry of the three-coordinate fluoride complex **2** in diethyl ether with 1 molar equiv of $Et_2O{\cdot}BF_3$ results in dissolution of the material (Scheme 3b). Slow evaporation of solvent gives crystalline $L^{tBu}Fe(OEt_2)(\eta^1\text{-}BF_4)$ (**3**), for which the X-ray crystal structure is shown in Figure 5a. The structure of **3** shows that the BF_4^- anion lies in the pseudoaxial position and the molecule has a relatively low pyramidal distortion with $\tau = 0.13$ (Table 2). The Fe−F distance in **3** is 2.0672(10) Å, whereas the $B-F_{bound}$ distance is 1.488(2) Å, roughly 10% longer than the mean $B-F_{free}$ distance of 1.349(5) Å (Table 2). Therefore the BF_4^- anion is strongly activated based on the definition of Roesky et al.[10a] Still, the BF_4^- anion dissociates readily in solution: the ^{19}F NMR spectrum of **3** in THF shows a single resonance at 155.1 ppm (vs $CFCl_3$), virtually the same as that of $Na^+BF_4^-$ (see Experimental Section). The complete abstraction of the fluoride ligand in **2** suggests that *although the* $Fe^{II}-F$ *bond is very short, it can be activated by Lewis acids.*

Transition metal fluorides have been used as precursors to other species by exploiting the silaphilicity of the fluoride ligand.[10,28] In agreement with this idea, $\mathbf{1_2}$ and **2** react with silyl compounds to generate new complexes, in reactions that are driven by the formation of very strong Si−F bonds. Thus, the reaction of equimolar amounts of $[L^{Me}FeF]_2$ and hexamethyldisilathiane (HMDS) proceeds smoothly in a couple of hours at 60 °C in toluene to give the diiron(II) sulfide $L^{Me}Fe(\mu\text{-}S)FeL^{Me}$ (Scheme 3c), which we have synthesized independently.[16] Under similar reaction conditions, the fluoride complex **2** reacts partially with 0.5 equiv of HMDS to give a 1:1 mixture (as observed by ^1H NMR in C_6D_6) of a product tentatively assigned as the analogous diiron(II) sulfide $L^{tBu}Fe(\mu\text{-}S)FeL^{tBu}$, along with the new compound $L^{tBu}FeSSiMe_3$ (**4**) (Scheme 3c). The trimethylsilylthiolate complex **4** is isolated in 86% yield, and its X-ray crystal structure is shown in Figure 5c (see also Table 3).

The reaction of $L^{tBu}FeF$ with 2 equiv of bis(trimethylsilyl)acetylene ($Me_3SiCCSiMe_3$) provides complex $L^{tBu}FeCCSiMe_3$ (**5**) in 61% isolated yield (Scheme 3d). The molecular structure of **5** is shown in Figure 5d (see also Table 3). New routes to paramagnetic complexes of transition metals containing sp-hybridized hydrocarbyl ligands are of interest due to the potential ability of such materials to act as molecular wires.[29]

Triethylsilane (Et_3SiH) also reacts with the iron(II) fluoride complexes, providing a convenient synthetic route to the hydride complexes $[L^{Me}FeH]_2$ ($\mathbf{6_2}$) and $[L^{tBu}FeH]_2$ ($\mathbf{7_2}$) (Scheme 3e). The

(28) (a) Hoffman, N. W.; Prokopuk, N.; Robbins, M. J.; Jones, C. M.; Doherty, N. M. *Inorg. Chem.* **1991**, *30*, 4177−4181. (b) Doherty, N. M.; Critchlow, S. C. *J. Am. Chem. Soc.* **1987**, *109*, 7906−7908.

Table 3. Structural Characterization of Complexes Prepared from Iron(II) Fluorides and Silyl Compounds: Bond Distances (Å) and Angles (deg)

$L^{tBu}FeSSiMe_3$ (**4**)		$L^{tBu}FeCCSiMe_3$ (**5**)		$[L^{Me}Fe(\mu\text{-}H)]_2$ (**6_2**)	
Fe−S	2.2487(12), 2.2460(12)	Fe−C	1.961(6)	Fe−H	1.40(9), 1.45(8), 1.55(8), 1.56(9)[a]
Fe−N	1.964−1.981	Fe−N	1.953(4), 1.964(4)	Fe−N	1.971(4), 1.975(4), 1.978(4), 1.988(4)
S−Si	2.1100(16), 2.0991(16)	C−C	1.226(6)	Fe···Fe	2.4638(11)
Fe−S−Si	118.29(6), 117.90(6)	N−Fe−C	141.07(18), 124.11(18)	Fe−H−Fe	111(4), 113(4)[a]
N−Fe−N	95.30(13), 94.32(12)	N−Fe−N	94.81(16)	N−Fe−N	95.0(2), 95.0(2)
C−N−C	126.1−126.7	C−N−C	127.9(4), 128.1(4)	C−N−C	117.8(4), 117.9(4), 119.3(4), 119.5(4)

[a] Iron-bound hydrogen atoms (**6_2**) were located in the electron density map and refined with isotropic thermal parameters.

Scheme 4

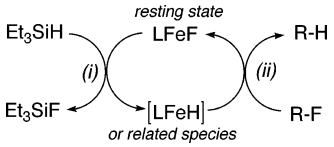

latter complex has been synthesized independently, and its properties and some of its reactivity have been reported.[17] Compounds **6_2** (μ_{eff} = 4.0(3) μ_B) and **7_2** (μ_{eff} = 3.8(3) μ_B)[17] are among the very few characterized paramagnetic hydride complexes in the literature.[17,30,] The new compound **6_2** is isolated in 89% yield, and its X-ray crystal structure is shown in Figure 5b (see also Table 3). Its properties and reactivity will be the subject of future publications.

Similarly to the fluoride complexes **1_2** and **2**, the four-coordinate fluoride complexes such as **1·^{t}Bupy** or **2·^{t}Bupy** (see above) react with triethylsilane to give the corresponding four-coordinate hydride complexes (complete conversion by ^{1}H NMR), which are similar to the recently reported $L^{tBu}FeH$(4-^{t}Bu-py).[17] The driving force for all the reactions between the fluoride complexes and silyl reagents is clearly the formation of a very strong Si−F bond (159 kcal/mol),[2,31] which renders the reactions enthalpically favorable. *The Fe^{II}−F bond is thus silaphilic*, making the fluoride complexes valuable synthetic precursors for new molecules with a variety of ligands.

Envisioning a Catalytic Cycle for Hydrodefluorination. We have previously observed that low-coordinate iron hydride complexes are capable of breaking strong bonds to electronegative elements,[17] suggesting that they might be active toward C−F activation reactions. Because the iron(II) fluoride complexes react with Et_3SiH to give iron(II) hydrides, this could lead to *catalytic* C−F bond activation (Scheme 4). However, there is no evidence of reaction when the hydride complexes **6_2** and **7_2** are heated at 120 °C for one week in C_6D_6 or THF-d_8 with hexafluorobenzene (C_6F_6) or octafluorotoluene ($C_6F_5CF_3$), as monitored by ^{19}F and ^{1}H NMR. Nevertheless, when these reactions are repeated *in the presence of triethylsilane, C−F activation takes place, giving in each case the product of monohydrodefluorination (HDF)*: pentafluorobenzene (C_6F_5H) or heptafluorotoluene (*p*-H-$C_6F_4CF_3$), respectively. The formation of fluorotriethylsilane ($FSiEt_3$) is also observed (^{19}F NMR, GC-MS). Thus, while direct reaction of fluorinated aromatics with the iron(II) hydride complexes does not occur, *C−F activation becomes feasible in the presence of silane as a fluoride trap*.

Although Scheme 4 shows a simple conceptual explanation for HDF catalysis, it is incomplete because the hydride complex does not directly react with fluorinated aromatic compounds. The way in which the silane assists the hydride complex is uncertain. However, the intermediacy of the hydride complex cannot be ruled out since both fluoride and hydride complexes are able to carry out the HDF reaction in the presence of silane.

Catalytic Perfluoroarene Hydrodefluorination. The hydrodefluorination (HDF) of aromatic perfluorocarbons is achieved when a stoichiometric mixture of triethylsilane and an aromatic perfluorocarbon is heated in the presence of 0.2 molar equiv of **1_2**, **2**, **6_2**, or **7_2** (Table 4).[32] Conversions are higher when starting with fluorides rather than hydrides (see below) and higher with the monomeric fluoride **2** than with the dimeric **1_2**, as shown for hexafluorobenzene (Table 4, entries 1 and 2). The highest activities among the aromatic substrates are observed for octafluorotoluene (TON = 4.5) and perfluoropyridine (TON = 3.6), and HDF activity decreases as a function of the degree of fluorination on the substrate. The extent of HDF activity correlates with the electron affinity of the perfluoroarene (Figure 6),[33] a feature that has been identified previously in some C−F activation schemes.[7c,33] Other aromatic substrates with low fluorine substitution such as *para*-fluorotoluene, α,α,α-trifluorotoluene, or 1,3-bis(trifluoromethyl)benzene do not undergo C−F activation under the reaction conditions described above. However, only substrates containing sp^2 carbons undergo C−F activation (fluorinated alkenes are discussed below). No benzylic C−F activation is observed in octafluorotoluene. Similarly, perfluorinated methylcyclohexane (containing only aliphatic C−F bonds) does not undergo hydrodefluorination despite having one of the highest electron affinities known for a perfluorocarbon (1.06 eV).[33b] Therefore, a high electron affinity does not suffice for HDF to occur in the presence of the iron catalyst, and only unsaturated substrates are activated.

(29) (a) Rosenthal, U. *Angew. Chem., Int. Ed.* **2003**, *42*, 1794−1798. (b) Roué, S.; Lapinte, C.; Bataille, T. *Organometallics* **2004**, *23*, 2558−2567. (c) Berry, J. F.; Cotton, F. A.; Murillo, C. A. *Organometallics* **2004**, *23*, 2503−2506. (d) Mironov, V. S.; Chibotaru, L. F.; Ceulemans, A. *J. Am. Chem. Soc.* **2003**, *125*, 9750−9760. (e) Stang, S. L.; Paul, F.; Lapinte, C. *Organometallics* **2000**, *19*, 1035−1043. (f) Gu, X. *Organometallics* **1998**, *17*, 5920−5923.

(30) (a) Poli, R. *Chem. Rev.* **1996**, *96*, 2135−2204. (b) Bruckhardt, U.; Casty, G. L.; Tilley, T. D.; Woo, T. K.; Rothlisberger, U. *Organometallics* **2000**, *19*, 3830−3841. (c) Kupfer, V.; Thewalt, U.; Horacek, M.; Petrusova, L.; Mach, K. *Inorg. Chem. Commun.* **1999**, *2*, 540−544. (d) Jewson, J. D.; Liable-Sands, L. M.; Yap, G. P. A.; Rheingold, A. L.; Theopold, K. H. *Organometallics* **1999**, *18*, 300−305. (e) Hessen, B.; Van Bolhuis, F.; Teuben, J. H.; Petersen, J. L. *J. Am. Chem. Soc.* **1988**, *110*, 295−296. (f) Bianchini, C.; Mealli, C.; Meli, A.; Sabat, M. *J. Chem. Soc., Chem. Commun.* **1986**, 777−779. (g) Raynor, J. B. Sattelberger, A. P.; Luetkens, M. L. *Inorg. Chim. Acta* **1986**, *113*, 51−54. (h) Luetkens, M. L. Elcesser, W. L. Huffman, J. C. *Inorg. Chim. Acta* **1984**, *23*, 1718−1726.

(31) Brook, M. A. *Silicon in Organic, Organometallic and Polymer Chemistry*; Wiley: New York, 2000; pp 28−38.

(32) In the absence of iron fluoride or hydride there was no sign of reaction (= 1%) between any of the substrates and trisubstituted silanes.

(33) (a) Dillow, G. W.; Kebarle, P. *J. Am. Chem. Soc.* **1989**, *111*, 5592−5596. (b) Kebarle, P.; Chowdhury, S. *Chem. Rev.* **1987**, *87*, 513−534. (c) Wentworth, W. E.; Limero, T.; Chen, E. C. M. *J. Phys. Chem.* **1987**, *91*, 241−245. (d) Chowdhury, S.; Grimsrud, E. P.; Heinis, T.; Kebarle, P. *J. Am. Chem. Soc.* **1986**, *108*, 3630−3635.

Table 4. Catalytic Hydrodefluorination (HDF) of Fluorocarbons with Iron(II) Diketiminate Complexes

	precatalyst conc, M	substrate conc, M	solvent	reagent conc, M	conditions	product distribution	selectivity[a] (%)	TON[b]
1	**1₂**, 0.021	C_6F_6, 0.11	THF-d_8	Et_3SiH, 0.11	45 °C, 4 days	C_6HF_5 (20%) p-$C_6H_2F_4$ (0.2%)	99	1.0
2	**2**, 0.021	C_6F_6, 0.11	THF-d_8	Et_3SiH, 0.11	45 °C, 4 days	C_6HF_5 (50%) p-$C_6H_2F_4$ (0.8%)	98	2.5
3	none	C_6F_6, 0.11	THF-d_8	$KHBEt_3$, 0.11	RT, 5 min	C_6HF_5 (79%) p-$C_6H_2F_4$ (14%)	84	
4	**2**, 0.021	C_6F_6, 0.11	THF-d_8	Et_3SiH, 0.11	80 °C, 4 days	C_6HF_5 (24%)	100	1.2
5	**2**, 0.021	C_6F_6, 0.11	C_6D_6	Et_3SiH, 0.11	45 °C, 4 days	C_6HF_5 (6%)	100	0.3
6	**2**, 0.021	C_6F_5H, 0.11	THF-d_8	Et_3SiH, 0.11	45 °C, 4 days	p-$C_6H_2F_4$ (4%)	100	0.2
7	**2**, 0.021	$C_6F_5CF_3$, 0.11	THF-d_8	Et_3SiH, 0.11	45 °C, 12 h	p-$C_6HF_4CF_3$ (90%)	100	4.5
8	**2**, 0.021	C_5F_5N, 0.11	THF-d_8	Et_3SiH, 0.11	45 °C, 4 days	p-C_5HF_4N (71%)	100	3.6
9	**1₂**, 0.010	CF_2=$CFCF_3$, 0.11[c]	THF-d_8	Et_3SiH, 0.11	100 °C, 3 h.	CHF=$CFCF_3$ (*E*: 60%, *Z*: 27%), CF_2=$CHCF_3$ (2%)	67	9.8
10	**1₂**, 0.010	CH_2=$CHCF_3$, 0.11[c]	THF-d_8	Et_3SiH, 0.11	100 °C, 4 days	CF_2=$CHCH_3$ (11%)	100	1.2

[a] Selectivity for the main hydrodefluorination product. [b] TON = moles of products (overall)/moles of catalyst. Precision limits are ±4% of the given value. [c] Total concentration (see Experimental Section for details).

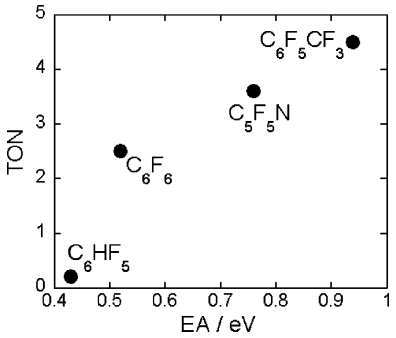

Figure 6. Plot of hydrodefluorination activity vs perfluoroarene electron affinity.

Because turnovers are higher than 1 and because the catalyst is introduced in the form of a fluoride complex, *these reactions are truly catalytic*. The activity observed is dependent on the solvent, with THF ($\epsilon = 7.6$)[34] giving higher conversions than the less polar solvent toluene ($\epsilon = 2.3$).[34] The reactions also proceeded in dry pyridine as solvent ($\epsilon = 12.4$),[34] but the conversions achieved were intermediate between those in THF and benzene.[35]

The perfluoroarene HDF reactions catalyzed by **2** are regioselective, with C−F activation at the position *para* to the most electron-withdrawing group always observed. Interestingly, attempts to carry out HDF of p-$HC_6F_4CF_3$ (heptafluorotoluene) fail even after prolonged heating. The HDF reactions are highly chemoselective as well, since mainly mono-hydrodefluorination products and only traces of double HDF products are observed. For example, the iron-catalyzed HDF of C_6F_6 gives C_6HF_5 with 98% selectivity, while direct reaction of C_6F_6 with the strong reducing agent $KHBEt_3$[36] gives a lower selectivity of the mono-HDF product, 84% (entries 2 and 3 of Table 4).

Choice of Silane and Catalyst Deactivation. Some differences are evident when the temperature of reaction and the fluoride acceptor are varied. When triethylsilane is used, the best conversion is observed at a temperature of 45 °C, with higher temperatures resulting in faster catalyst decomposition (entries 2 and 4). When phenylsilane ($PhSiH_3$) is used, complete decomposition ensues at room temperature and no C−F activation is observed. Changing the electronic environment at the silicon center affects both the catalyst stability and the HDF rate. The following order of reactivity is evident for different trisubstituted silanes, expressed in terms of conversion of hexafluorobenzene (0.11 M) in THF-d_8 at 60 °C with 20 mol % catalyst loading: $(EtO)_3SiH$ (41%, 5 min), Ph_3SiH (22%, 12 h), 3,5-$(CF_3)_2C_6H_3$-$SiHMe_2$ (92%, 4 days), Et_3SiH (complete in 4 days). Thus, while triethoxysilane reacts at room temperature, it also leads to the most rapid catalyst deactivation (accompanied by precipitate formation).[32] H_2 gas is not an effective reductant at pressures of 250−1500 psi, even with added traps for HF such as Et_3N, py, and NaF.

The hydride complex **7₂** also catalyzes HDF, although the conversion was lower. Catalyst decay was faster in this case, offering a likely explanation for the difference in catalytic activity. Control experiments show that heating a solution of hydride complex **6₂** or **7₂** in THF-d_8 in the presence of the silane leads to decomposition, and multiple unidentified paramagnetically shifted peaks are evident in the ^1H NMR spectra.

Kinetics of Perfluoroarene Hydrodefluorination. Because of catalyst decomposition, we are not able to follow the HDF reaction kinetics to completion and turned to kinetic inquiry using the initial rate method.[37] In a typical kinetics experiment, the initial concentration of substrate (octafluorotoluene), silane, or **2** is varied while the other two are kept constant relative to a reference experiment ($[Et_3SiH]_0 = [C_6F_5CF_3]_0 = 0.11$ M, $[\mathbf{2}]_0 = 0.02$ M in THF-d_8 at 341 K). The disappearance of substrate and formation of a hydrodefluorination product are monitored by ^{19}F NMR. Figure 7 and Table 5 show the initial rates from these experiments. The initial rate has a first-order dependence on silane concentration and on iron concentration, but it is independent of the concentration of octafluorotoluene.

$$d[p\text{-}C_6HF_4CF_3]/dt = k[Et_3SiH]^1[L^{tBu}FeF]^1[C_6F_5CF_3]^0 \quad (1)$$

The second-order rate constant derived from this rate equation is $k = 1.4(1) \times 10^{-3}$ M^{-1} s^{-1}. There is a small normal kinetic isotope effect with deuteration of the silane, $k^{SiH}/k^{SiD} = 1.4(1)$ (entry 5 in Table 5 and Figure 7). Finally, the rate of HDF is

(34) Dielectric constant: Kerr, J. A. In *CRC Handbook of Chemistry and Physics*, 71st ed.; Lide, R. L., Ed.; CRC Press: Boca Raton, FL, 1990; p 8−44.
(35) The HDF reaction does not take place in more polar solvents such as DMF or HMPA. This may be due to reaction between the iron(II) hydride complex and these solvents.
(36) Fryzuk, M. D.; Lloyd, B. R.; Clentsmith, G. K. B.; Rettig, S. J. *J. Am. Chem. Soc.* **1994**, *116*, 3804−3812.
(37) Espenson, J. H. *Chemical Kinetics and Reaction Mechanisms*, 2nd ed.; McGraw-Hill: New York, 1995.

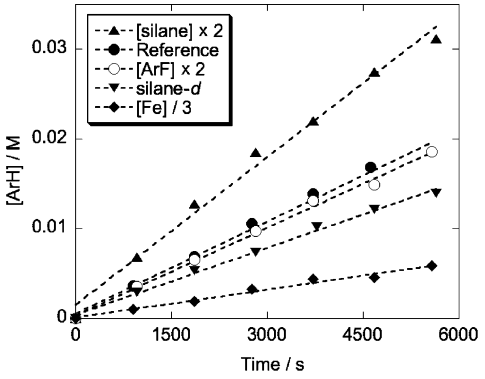

Figure 7. Time course of octafluorotoluene hydrodefluorination, showing changes in the initial observed rates vs a reference experiment with $[\text{silane}]_0 = [C_6F_5CF_3]_0 = 0.11$ M, $[\text{Fe}]_0 = 0.02$ M, using THF-d_8 at 341 K.

Table 5. Hydrodefluorination of Octafluorotoluene with Triethylsilane in THF-d_8, Initial Rates[a]

entry	initial concentrations (M) $[Et_3SiH]_0$	$[C_6F_5CF_3]_0$	$[L^{tBu}FeF]_0$	initial rate (10^{-6} M s^{-1})
1	0.11	0.11	0.021	3.38(4)
2	0.11	0.22	0.021	3.30(4)
3	0.22	0.11	0.021	5.53(4)
4	0.11	0.11	0.0072	1.2(1)
5	Et_3Si**D**: 0.11	0.11	0.021	2.43(5)
6, added 47 mM DHA	0.11	0.11	0.021	2.9(1)

[a] Data for first 100 min (≤39% conversion).

only slightly affected by addition of an excess amount of dihydroanthracene (DHA, entry 6 in Table 5).

During the course of the experiments, the only iron species detected by ^{1}H NMR is **2**, indicating the fluoride complex is the resting state of the catalyst. It is possible that the active species is a form of the hydride complex, which quickly reacts with the relative excess of perfluorocarbon and silane under the reaction conditions.

HDF of Aromatic Perfluorocarbons: Mechanistic Considerations. The apparent rate law, the H/D kinetic isotope effect, and the observation of **2** as the resting state each suggests that the rate-limiting step in the HDF of octafluorotoluene is reaction of the iron fluoride complex with silane. The reaction of $L^{tBu}FeF$ with silane is expected to form $\mathbf{7_2}$, a hydride complex that is known to be very reactive (it even cleaves the N=N bond of azobenzene).[17] It seems reasonable that this low-coordinate iron hydride could also reduce C−F bonds. This is supported by the fact that the hydride complex $\mathbf{7_2}$ can be used instead of **2** as a catalyst, although conversions are lower due to more rapid catalyst decomposition.

However, some observations are inconsistent with the simple pathway shown in Scheme 4. First, neither $\mathbf{7_2}$ nor $\mathbf{6_2}$ stoichiometrically hydrodefluorinates fluoroaromatics in the absence of silane (see above). This is not due to an unfavorable equilibrium constant, because aromatic compounds do not react with the iron(II) fluoride complexes. This suggests that the hydride alone is not directly responsible for C−F activation and the actual catalytic species is more complicated, perhaps a silane adduct of the hydride.[38] Additionally, unless the mechanism changes or step *(i)* is not rate-limiting for all substrates, then there should be identical rates with different fluorinated substrates, contrary to our observations. Therefore, *the simple model in Scheme 4 is not a satisfactory mechanistic explanation and should be viewed as only a working model.* Unfortunately, the apparent competition between catalyst decomposition and catalytic HDF hinders our ability to query the mechanism in more detail with this system. While a more complete explanation will await a more robust catalyst, it is possible to narrow down the mechanistic possibilities based on the currently available data.

All of the perfluoroarene HDF reactions occur without an induction period, suggesting that autocatalysis by a reaction byproduct such as fluoride anion[4b] is unlikely. Repeated distillation of the starting materials, different batches of iron catalyst, addition of a drop of mercury, or different reaction vessel materials (glass or Teflon) had little effect on the reaction rate, also arguing against catalysis by a trace impurity. Neither $L^{tBu}FeCl$,[15f] $L^{tBu}FeCH_2{}^tBu$,[18c] nor $L^{tBu}FeMe$[15c] catalyzed the HDF reaction.

Hydrodefluorination of octafluorotoluene under standard conditions (60 °C, 19 h) with and without dihydroanthracene (DHA), a common radical trap, gives nearly the same extent of conversion to p-$C_6HF_4CF_3$ (46% and 54%, respectively).[39] In an analogous experiment with 20 mM **2**, 110 mM Et_3SiH, and 47 mM DHA, the derived rate constant is $k = 1.2(1) \times 10^{-3}$ M^{-1} s^{-1}, statistically the same as that in the absence of the radical trap (Table 5).[40] Other workers have ruled out a radical path for C−F activation reactions based on similar observations.[4a,b,1]

A pathway involving oxidative addition to $\mathbf{7_2}$ or another Fe^{II} complex would form an iron(IV) complex. Such a high-valent intermediate is unprecedented in diketiminate-iron complexes.[15−18] In addition, a five-coordinate intermediate would suffer from severe steric congestion as a consequence of the hindering diketiminate ligand. An oxidative addition pathway is also inconsistent with the fact that H_2 gas (possibly the most active substrate toward oxidative addition)[42] does not function as a competent reductant, nor does H_2 add to other iron(II) diketiminate complexes.[15−18,43]

The dependence of catalytic conversion on the substrate electron affinity suggests the possibility of a mechanism involving rate-limiting electron transfer from iron(II) to fluoroarene.[44,45] Therefore, the redox properties of the putative intermediate iron-hydride complexes are relevant. The hydride complexes $\mathbf{7_2}$ and $\mathbf{6_2}$ are irreversibly oxidized at a potential of about −0.6 V vs ferrocene. Because perfluoroarenes have reduction potentials of −2.5 to −3.0 V vs ferrocene,[4b,46] electron transfer from iron to perfluoroarene is thus uphill by at least 1.8 V. Using this energy as the minimum value for $\Delta G^{\ddagger}_{ET}$, a

(38) Another possibility is that the active species is a silyl complex. Unfortunately, our several attempts to isolate a diketiminate iron(II) silyl complex independently have so far failed. The intermediacy of silyl cations (cf. ref 13) or silyl radicals is inconsistent with the regioselectivity of C−F activation and with the first-order dependence of the initial rate on iron concentration.

(39) A similar result is obtained when triphenylmethane (Ph_3CH, 0.47 molar equiv) is used as the radical trap (48% conversion under the same conditions).

(40) Separate experiments show that the hydride complex $\mathbf{7_2}$ slowly yields an undefined mixture of products (20−30% yield after 24 h at 60 °C) in the presence of DHA or Ph_3CH. Therefore, the slight decreases in HDF yield and rate caused by these radical scavengers may be attributed to a secondary reaction with the iron hydride complex. For example, hydride **6** can deprotonate acetonitrile, forming a dimeric alkyl complex $[L^{Me}Fe(\eta^1\text{-}CH_2\text{-}CN)]_2$.[18a]

(41) Whittlesey, M. K.; Perutz, R. N.; Moore, M. H. *Chem. Commun.* **1996**, 787−788.

(42) (a) Heinekey, D. M.; Lledós, A.; Lluch, J. M. *Chem. Soc. Rev.* **2004**, *33*, 175−182. (b) Kubas, G. J. *Metal Dihydrogen and σ-Bond Complexes: Structure, Theory and Reactivity*; Kluwer Academic/Plenum Publishers: New York, 2001.

simple analysis using the Eyring equation suggests that the rate for electron transfer from $\mathbf{7_2}$ to substrate would be no faster than 10^{-13} M^{-1} s^{-1}.[47] Therefore, outer-sphere electron transfer does not appear to be kinetically competent for perfluoroarene HDF. A similar conclusion was reached by Edelbach and Jones for the stoichiometric C−F activation of perfluoroarenes by $Cp^*Rh(PMe_3)H_2$.[4b]

Our experiments do not distinguish between other potential mechanisms. One such mechanism is nucleophilic aromatic substitution by a hydride ligand. This is consistent with the regioselectivity of HDF, which occurs *para* to electron-withdrawing groups. Alternatively, the reaction could proceed through an asynchronous σ-bond metathesis reaction involving a four-center transition state. To account for the effect of substrate electron affinity on the HDF, the C−F activation may involve the development of partial charges within the reaction pathway. We stress again that conclusive determination of the mechanism for HDF of fluoroaromatics will only be possible in a future system where the catalyst lifetime is improved.

Catalytic Hydrodefluorination of Fluoroolefins. The iron(II) fluoride $\mathbf{1_2}$ is also a precatalyst for the hydrodefluorination of fluorinated olefins (9.8 turnovers for hexafluoropropene and 1.2 turnovers for 3,3,3-trifluoropropene, Table 4). At 100 °C in THF, hexafluoropropene (0.11 M) quickly reacts with triethylsilane (0.11 M) in the presence of $\mathbf{1_2}$ (0.1 molar equiv), giving a mixture of C1 (87%, *E/Z* 2:1) and C2 (2%) hydrodefluorination products (Table 4, entry 9, Scheme 5). To our surprise, even 3,3,3-trifluoropropene undergoes HDF to give 1,1-difluoropropene as the main product (11% conversion in 4 days under similiar reaction conditions, entry 10).

There are many interesting differences between the HDF of fluoroaromatics and fluoroolefins by the iron fluorides: (1) The resting state observed by NMR during HDF of olefinic substrates has ^1H and ^{19}F resonances analogous to diketiminate iron(II) alkyl complexes (we have previously reported $L^{Me}FeCH_2CH_2CF_3$).[18a] In contrast, the fluoride complex (**2** or $\mathbf{1_2}$) is the observed resting state during HDF of perfluoroarenes. (2) The temperature required for olefinic C−F activation (100 °C) is considerably higher than the optimal temperature for the HDF of perfluoroarenes (45 °C, see above). (3) Only the L^{Me}-based fluoride $\mathbf{1_2}$ is active for HDF of perfluoroolefins, and **2** is inactive. This contrasts with aromatic HDF, in which $\mathbf{1_2}$ is less active than **2**. (4) The lack of selectivity for C1−F and C2−F activation in perfluoropropene contrasts with the high regioselectivity observed for the activation of aromatic substrates. (5) The hydrodefluorination of 3,3,3-trifluoropropene occurs through formal allylic C−F activation and despite this substrate having a lower degree of fluorination.

Scheme 5

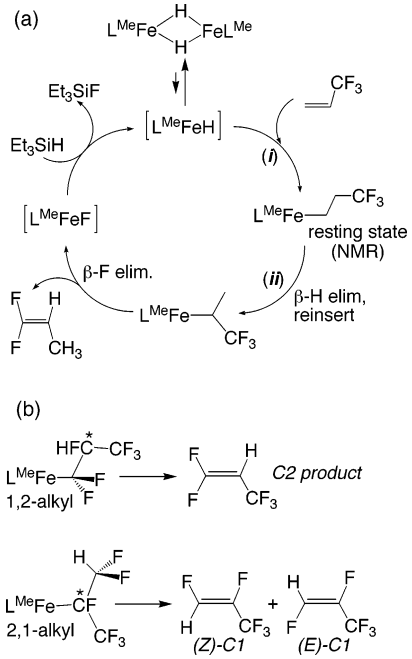

Thus, in comparison to fluoroaromatics, the HDF of fluoroolefins with the iron fluoride is more efficient with the *smaller* diketiminate, it is *less* regioselective, and it defluorinates more completely. All of these data are most consistent with a *hydride insertion/β-fluoride elimination mechanism for the HDF of perfluoroolefins* such as shown in Scheme 5.[48] We have extensively studied β-hydrogen elimination in diketiminate iron(II) alkyl complexes.[18] This work showed that hydride insertion into olefins rapidly generates alkyl complexes (step (*i*) in Scheme 5) and that β-hydrogen elimination occurs reversibly (step (*ii*)).[18] We have also shown that because of the higher steric hindrance of the larger diketiminate L^{tBu}, the alkyl complexes derived with this ligand undergo reversible insertion and β-hydrogen elimination much more slowly than complexes with the smaller ligand L^{Me}. The reproduction of these trends in the HDF of fluorinated alkenes indicates that an analogous mechanism is operative for hydrodefluorination of these substrates.

The intermediacy of fluorohydrocarbyl complexes is supported by experiments in which the putative intermediate $L^{Me}FeCH_2CH_2CF_3$[18a] is treated with triethylsilane. Interestingly, small amounts (up to 5% based on the alkyl complex) of $CF_2{=}CHCH_3$ are produced: this is the same product seen in the HDF of 3,3,3-trifluoropropene (Table 4, entry 10).[49] Although we previously have not observed β-F elimination in iron(II) diketiminates, the activation of C−F bonds in metal-bound fluoroalkyl ligands has been well documented.[3,50]

(43) Perfluorocarbon C−F bond oxidative addition is commonly preceded by well-defined and isolable fluorocarbon metal complexes. For example, Perutz and co-workers have characterized η^2-complexes of perfluoronaphthalene and perfluoropyridine (see ref 7b). In these nickel systems, C−F activation of perfluoropyridine occurred at C2 rather than at C4 as observed in the iron-catalyzed process demonstrated here. In our system, electronic absorption spectra show no substantial coordination of perfluorocarbons to the iron(II) diketiminate complex (see text and Figure 4).

(44) The selectivity for *para* C−F activation in C_6HF_5 has been explained by the relative radical character at this position in the radical anion.[41]

(45) (a) Yim, M. B.; Wood, D. E. *J. Am. Chem. Soc.* **1976**, *98*, 2053. (b) Shchegoleva, I. I.; Bilkis, I. I.; Schastnev, P. V. *Chem. Phys.* **1983**, *82*, 343.

(46) Marsella, J. A.; Glicinski, A. G.; Coughlin, A. M.; Pez, G. P. *J. Org. Chem.* **1992**, *57*, 2856−2860.

(47) There is a large disparity between the ability of perfluoroarenes to be reduced in the gas and solution phases. For example, the gas phase electron affinities of hexafluorobenzene and octafluorotoluene are favorable with values of 0.52(1) and 0.94(1) eV, respectively, but both have highly negative irreversible reduction potentials in THF solution (−3.0 and −2.95 V vs ferrocene; see refs 48 and 4b). In our mechanistic analysis, we use the solution values and assume that the overpotentials are not excessive (more than a few hundred millivolts).

(48) A similar hydride insertion/β-fluoride elimination mechanism is unlikely to operate in the HDF of perfluoroarenes. Such a mechanism would involve breaking the aromaticity of the substrate and therefore is expected to increase the activation barrier relative to olefinic C−F activation. This is inconsistent with HDF of perfluoroarenes occurring at lower temperatures than for olefinic substrates.

(49) Diketiminate iron(II) complexes without fluorinated hydrocarbyl ligands (e.g., $L^{Me}Fe^iBu$)[18] do not react with triethylsilane at 120 °C for 2 weeks. In a separate experiment, $[L^{Me}FeF]_2$ does not react with 1-hexene: we conclude that hydride formation must occur before catalysis proceeds.

Conclusions

Unprecedented three- and four-coordinate iron(II) fluorides can be isolated using the β-diketiminate ligands L^{Me} and L^{tBu}. These represent some of the first examples of discrete iron(II) fluoride complexes and the first example of a three-coordinate transition metal complex containing the fluoride ligand. The $Fe^{II}-F$ bond in these complexes is short, and they are very thermally robust. However, with suitable fluoride acceptors the compounds become reactive. For example, trialkylsilyl-substituted compounds lead to iron complexes with thiolate, acetylide, and hydride ligands, and $BF_3{\cdot}OEt_2$ removes the fluoride ligand.

Combining (a) the ability to transfer fluoride to silicon and (b) the high reactivity of the corresponding hydride complexes, it is possible to perform catalytic hydrodefluorinations. This process gives HDF of fluoroarenes and fluoroalkenes. There are few catalysts for homogeneously catalyzed C−F cleavage reactions,[11−13] and many in the literature that perform HDF are based on more expensive rhodium complexes.[12] Because the rhodium complexes are able to follow an oxidative addition mechanism, C−H activation competes with C−F activation. In contrast, the iron(II) complexes described here do not react with C−H bonds, perhaps because the first-row metal has a preference for M−F over M−H bonds.[50,51]

Despite the significance of the homogeneous iron-catalyzed HDF process described here, it is clear that major improvements are necessary. High catalyst loadings (20 mol %) are needed and the turnover numbers observed are low due to catalyst degradation at the temperatures needed for catalysis. This difficulty has also hindered mechanistic studies on the HDF reactions of perfluoroarenes. Our current mechanistic investigations indicate that the rate-limiting step for HDF of a perfluoroarene (octafluorotoluene) is the regeneration of the active hydrodefluorinating species from the iron fluoride and the silane. Although oxidative addition, as well as free-radical or other outer sphere electron transfer pathways are unlikely for perfluoroarene HDF, ruling out some of the remaining mechanisms will await a more robust or more rapid catalyst based on the discoveries demonstrated here. At this point, our working model is based on nucleophilic attack of hydride (in an unknown active species) on aromatic fluorocarbons. On the other hand, the evidence strongly supports a hydride insertion/β-fluoride elimination mechanism for olefinic HDF.

Experimental Section

General Considerations. Manipulations were performed under a nitrogen atmosphere by standard Schlenk techniques or in an M. Braun Unilab N_2-filled glovebox maintained at or below 1 ppm of O_2 and H_2O. Glassware was dried at 130 °C overnight. ^1H and ^{19}F NMR data were recorded on a Bruker Avance 400 MHz spectrometer at the specified temperature. ^1H shifts are reported in ppm, relative to residual protiated solvent in C_6D_6 (7.13 ppm) or THF-d_8 (3.58 ppm); relative integrations of peaks (and assignment when solved) are also given. ^{19}F shifts were referenced to α,α,α-trifluorotoluene (δ −63.73 ppm) and are reported against $CFCl_3$ (0 ppm). Solution magnetic susceptibilities were determined at 294 K by the Evans method.[52] Microanalyses were performed by Desert Analytics (Tucson, AZ). Vibrational spectra were recorded (450−4000 cm^{-1}) on KBr pellet samples in a Shimadzu Fourier transform infrared spectrophotometer (FTIR-8400S). A total of 64 scans at a 2 cm^{-1} resolution were collected in each case. Absorptions that were common among a pair ($[L^{Me}FeF]_2$ and $[L^{Me}FeCl]_2$, $L^{tBu}FeF$ and $L^{tBu}FeCl$) or series ($L^{tBu}FeF(L')$ or $L^{Me}FeF(L')$) of complexes were rejected on the grounds that they likely originate from the $L^{Me}Fe-$ fragment, rather than the Fe−F vibrations. Bands in the 450−1000 cm^{-1} region are thus reported according to their intensity (s = strong, m = medium, w = weak). Electronic spectra were recorded between 400 and 1100 nm with a Cary 50Bio UV−visible spectrophotometer, using quartz cuvettes of 1 cm optical path length. Pentane, diethyl ether, tetrahydrofuran (THF), toluene, and acetonitrile were purified by passage through activated alumina and "deoxygenizer" columns from Glass Contour Co. (Laguna Beach, CA). Deuterated benzene, tetrahydrofuran, and pyridine were dried over CaH_2, then over Na, and then vacuum distilled into storage containers or directly into an NMR tube. Hexamethyldisilathiane (HMDT), trimethyltin chloride, potassium fluoride (99+%), 3,3,3-trifluoropropene (99%), hexafluoropropene (99+%), and 4-phenylpyridine were purchased from Aldrich and used as received. Hexafluorobenzene, octafluorotoluene, pentafluorobenzene, pentafluoropyridine, *p*-heptafluorotoluene, triethylsilane, triethylsilane-*d*, triphenylsilane, dimethyl-3,5-bis(trifluoromethylphenyl)silane, triethoxysilane, 4-*tert*butylpyridine, pyridine, 4-trifluoromethylpyridine, and boron trifluoride diethyl etherate were dried over activated molecular sieves or vacuum distilled prior to use. Super-Hydride ($KHBEt_3$),[36] $L^{tBu}FeCl$,[15f] $[L^{Me}FeCl]_2$,[15a] $L^{Me}Fe(\mu\text{-}Cl)_2Li(THF)_2$,[15f] and all alkyl complexes such as $L^{Me}Fe$-*i*Bu and $L^{Me}FeCH_2CH_2CF_3$[18] were prepared by known procedures.

Synthesis of Trimethyltin Fluoride, Me_3SnF. Details reported on the preparation of Me_3SnF date back to the year 1918, and the reference is not widely available.[19] Thus we describe here our synthetic procedure. To a stirred solution of trimethyltin chloride (2 g, 10 mmol) in absolute ethanol (4 mL) was added dropwise a solution of KF (870 mg, 15 mmol) in deionized water (3 mL). The white precipitate was collected by filtration through a frit and washed with deionized water (1 mL), ethanol (1 mL), and diethyl ether (1 mL). The solid product was dried under high vacuum overnight before use (1.1 g, 61%).

$[L^{Me}Fe(\mu\text{-}F)]_2$ ($\mathbf{1_2}$). Trimethyltin fluoride (240 mg, 1.32 mmol), $L^{Me}Fe$-*i*Bu (600 mg, 1.2 mmol), and toluene (8 mL) were placed in a resealable Schlenk bomb with a stir bar. The mixture was stirred and heated to 80 °C overnight. After cooling the mixture to room temperature and allowing the precipitate to settle, the soluble fraction was filtered through Celite in a frit. After solvent removal under vacuum a green solid was obtained, which was recrystallized from diethyl ether (490 mg, 83% yield). Anal. Found (calcd): C, 70.75 (70.72), H, 8.63 (8.39), N, 5.62 (5.69). μ_{eff} (per dimer; C_6D_6, 21 °C) = 6.2(3) μ_B. ^1H NMR (C_6D_6, 21 °C): 14.0 (1H, α-CH), 5.2 (4H, *m*-CH), 2.0 (12H, $^iPr-CH_3$), −10 (4H, ^iPr-CH), −11.7 (6H, CH_3-L), −46.3 (2H, *p*-CH), −51.0 (12H, $^iPr-CH_3$). The ^{19}F NMR of $\mathbf{1_2}$ showed no resonances between 500 and −500 ppm. No IR bands corresponding to the Fe−F bond vibrations were observed, and the IR spectra of $\mathbf{1_2}$ and $[L^{Me}FeCl]_2$ were nearly identical. Vis (toluene): 397 nm (3600 M^{-1} cm^{-1}), 455 nm (560 M^{-1} cm^{-1}), 791 nm (90 M^{-1} cm^{-1}).

$L^{tBu}FeF$ (2). Trimethyltin fluoride (300 mg, 1.6 mmol), $L^{tBu}FeMe$[15c] (1.02 g, 1.8 mmol), and toluene (20 mL) were placed in a resealable flask and heated to 80 °C while stirring overnight. Then the solvent was evaporated under vacuum, and the solid residue washed with pentane (5 × 5 mL). After vacuum-drying a pink powder was obtained (760 mg, 74%). Crystals for X-ray diffraction were grown by cooling a saturated toluene solution from 80 °C to room temperature. Anal. Found (calcd): C, 72.37 (72.90), H, 8.96 (9.26), N, 4.71 (4.86). μ_{eff} (toluene-d_8, 21 °C) = 5.6(3) μ_B. ^1H NMR (toluene-d_8, 21 °C): 42.1 (18H, $(CH_3)_3C-L$), −27.0 (2H, *m*-CH), −31.1 (12H, $^iPr-CH_3$), −98.5 (2H, *p*-CH), −113.5 (16H, $^iPr-CH_3$, ^iPr-CH). The ^{19}F NMR of **2** in toluene-d_8 or THF-d_8 showed no resonances between 500 and −500

(50) (a) Kraft, B. M.; Lachicotte, R. J.; Jones, W. D. *Organometallics* **2002**, *21*, 727−731. (b) Clot, E.; Mégret, C.; Kraft, B. M.; Eisenstein, O.; Jones, W. D. *J. Am. Chem. Soc.* **2004**, *126*, 5647−5653. (c) Gérard, H.; Eisenstein, O.; *Dalton Trans.* **2003**, 839−845. (d) Strazisar, S. A.; Wolczanski, P. T. *J. Am. Chem. Soc.* **2001**, *123*, 4728−4740.
(51) (a) Reinhold, M.; McGrady, J. E.; Perutz, R. N. *J. Am. Chem. Soc.* **2004**, *126*, 5268−5276.
(52) (a) Schubert, E. M. *J. Chem. Educ.* **1992**, *69*, 62. (b) Evans, D. F. *J. Chem. Soc.* **1959**, 2003−2005.

ppm. IR (KBr pellet, cm^{-1}): 596 (s, ν_{Fe-F}). Vis (toluene): 530 nm (730 M^{-1} cm^{-1}), 715 nm (100 M^{-1} cm^{-1}).

Formation of Four-Coordinate Fluoride Complexes. The substituted pyridine (0.2 mmol) or acetonitrile (1.0 mmol) was added to the fluoride complex $\mathbf{1_2}$ (100 mg, 0.1 mmol) or **2** (115 mg, 0.2 mmol) in diethyl ether (5 mL). Each individual product was isolated by crystallization from these solutions at −38 °C. **L^{Me}FeF(4-^{t}Bu-py) (1·'Bupy)**: 87% yield. Anal. Found (calcd): C, 72.19 (72.71), H, 8.93 (8.67), N, 7.12 (6.69). μ_{eff} (C_6D_6, 21 °C) = 5.1(3) μ_B. ^{1}H NMR (C_6D_6, 21 °C): 36.4 (4H, *m*-CH), 20.8 (2H, *o*-CH-py), 16.8 (2H, *m*-CH-py), 1.5 (12H, ^{i}Pr−CH_3), −2.5 (12H, ^{i}Pr−CH_3), −6.8 (4H, ^{i}Pr−CH), −12.2 (9H, $(CH_3)_3$C−py), −38.5 (2H, *p*-CH), −64.0 (1H, α-CH), −86.3 (6H, $(CH_3)_2$−L). IR (KBr pellet, cm^{-1}): 717 (m, ν_{Fe-F}). Vis (toluene): 425 nm (2180 M^{-1} cm^{-1}), 465 nm (1260 M^{-1} cm^{-1}), 946 nm (150 M^{-1} cm^{-1}). **L^{Me}FeF(4-CF_3-py) (1·CF_3py)**: 68% yield. Anal. Found (calcd): C, 65.96 (65.73), H, 7.12 (7.09), N, 6.61 (6.57). μ_{eff} (C_6D_6, 21 °C) = 5.1(3) μ_B. ^{1}H NMR (C_6D_6, 21 °C): 21.0 (2H, *o*-CH-py), 20.3 (4H, *m*-CH), 10.0 (2H, *m*-CH-py), 1.1 (12H, ^{i}Pr−CH_3), −9.3 (12H, ^{i}Pr−CH_3), −39.2 (2H, *p*-CH), −51.0 (4H, ^{i}Pr−CH), −69.0 (1H, α-CH), −87.8 (6H, $(CH_3)_2$−L). IR (KBr pellet, cm^{-1}): 717 (w), 669 (s, ν_{Fe-F}), 609 (m), 557 (m). Vis (toluene): 401 nm (1930 M^{-1} cm^{-1}), 512 nm (670 M^{-1} cm^{-1}), 898 nm (120 M^{-1} cm^{-1}). **L^{tBu}FeF(4-^{t}Bu-py) (2·'Bupy)**: 95% yield. Anal. Found (calcd): C, 74.45 (74.24), H, 8.68 (9.35), N, 5.82 (5.90). μ_{eff} (C_6D_6, 21 °C) = 5.0(3) μ_B. ^{1}H NMR (C_6D_6, 21 °C): 38.0, 21.8, 7.9, 2.0, 1.1, −2.3, −46.5, −88.0. IR (KBr pellet, cm^{-1}): 544 (s, ν_{Fe-F}). Vis (toluene): 462 nm (2110 M^{-1} cm^{-1}), 968 nm (150 M^{-1} cm^{-1}). **L^{tBu}FeF($NCCH_3$) (2·ACN)**: 61% yield. Anal. Found (calcd): C, 71.44 (71.94), H, 9.56 (9.14), N, 7.02 (6.80). μ_{eff} (C_6D_6, 21 °C) = 4.9(3) μ_B. ^{1}H NMR (C_6D_6, 21 °C): 21.4, 17.4, 12.0, 7.9, 1.0, −4.3, −13.9, −49.8, −85.1. IR (KBr pellet, cm^{-1}): 538 (s, ν_{Fe-F}). Vis (toluene−acetonitrile, 10:1 v/v): 457 nm (1040 M^{-1} cm^{-1}), 920 nm (150 M^{-1} cm^{-1}). The following adducts were observed spectroscopically: **[L^{Me}FeF(py)]** ^{1}H NMR (C_6D_6, 21 °C): 35.0 (5H, *o*-, *p*-, *m*-CH-py), 19.0 (4H, *m*-CH), 2.1 (12H, ^{i}Pr−CH_3), −10.0 (16H, ^{i}Pr−CH, ^{i}Pr−CH_3), −38.7 (2H, *p*-CH), −68.1 (1H, α-CH), −87.2 (6H, $(CH_3)_2$−L). IR (KBr pellet, cm^{-1}): 704 (s, ν_{Fe-F}). Vis (toluene): 432 nm (1630 M^{-1} cm^{-1}), 468 nm (1110 M^{-1} cm^{-1}), 944 nm (130 M^{-1} cm^{-1}). **[L^{Me}FeF(4-Ph-py)]** ^{1}H NMR (C_6D_6, 21 °C): 36.0 (4H, *m*-CH), 21.0 (2H, *o*-CH-py), 17.3 (2H, *m*-CH-py), 11.5 (1H, *p*-CH−Phpy), 10.7 (2H, *m*-CH−Phpy), 3.3 (2H, *o*-CH−Phpy), 1.3 (12H, ^{i}Pr−CH_3), −6.6 (4H, ^{i}Pr−CH), −12.1 (12H, ^{i}Pr−CH_3), −38.6 (2H, *p*-CH), −66.0 (1H, α-CH), −86.8 (6H, $(CH_3)_2$−L). IR (KBr pellet, cm^{-1}): 733 (w), 690 (m, ν_{Fe-F}), 623 (w), 544 (m). Vis (toluene): 411 nm (1840 M^{-1} cm^{-1}), 480 nm (1960 M^{-1} cm^{-1}), 943 nm (210 M^{-1} cm^{-1}). **[L^{tBu}FeF(py)]** ^{1}H NMR (C_6D_6, 21 °C): 39.5, 20.0, 7.3, 2.5, 1.2, −3.6, −47.3, −87.2. IR (KBr pellet, cm^{-1}): 540 (s, ν_{Fe-F}). Vis (toluene): 467 nm (2070 M^{-1} cm^{-1}), 965 nm (160 M^{-1} cm^{-1}). **[L^{tBu}FeF(THF)]** ^{1}H NMR (THF-d_8, adduct, 21 °C): 28.0 (1H, CH_3-L), 27.4 (18H, $(CH_3)_3$C−L), −4.0 (12H, ^{i}Pr−CH_3), −25.4 (4H, *m*-CH), −50.6 (12H, ^{i}Pr−CH_3), −57.5 (2H, *p*-CH), −69.7 (4H, ^{i}Pr−CH). Vis (THF): 464 nm (930 M^{-1} cm^{-1}), 979 nm (120 M^{-1} cm^{-1}).

L^{tBu}FeOEt_2(η^1-BF_4) (3). $F_3B{\cdot}OEt_2$ (20 μL, 0.16 mmol) was added to a stirred suspension of **2** (92 mg, 0.16 mmol) in diethyl ether (3 mL), causing the immediate dissolution of the pink powder to form a yellow solution. Upon standing of this solution at −38 °C, **3** was obtained as yellow crystals (53 mg in two crops, 46%). Anal. Found (calcd): C, 65.01 (65.19), H, 8.17 (8.84), N, 3.99 (3.90). μ_{eff}(THF-d_8, 21 °C) = 4.6(3) μ_B. ^{1}H NMR (THF-d_8, 21 °C): 23.2, 15.2, 9.8, −23.0, −47.1, −51.3, −48.0, −70.0, −106.0. The ^{19}F NMR of **3** in THF-d_8 shows a single resonance that is identical to that seen for $Na^+BF_4^-$ (155.1 ppm), suggesting that complete dissociation of the BF_4^- anion occurs in solution.

Reaction of L^{tBu}FeF (2) with Hexamethyldisilathiane. Hexamethyldisilathiane (60 mg, 0.34 mmol, caution: STENCH!), **2** (100 mg, 0.17 mmol), and toluene (5 mL) were placed in a resealable flask and heated to 80 °C while stirring overnight. After thorough evaporation of solvent under vacuum, the material was dissolved in diethyl ether (3 mL) and cooled to −38 °C to give **4** (98 mg, 86%). Anal. Found (calcd): C, 68.83 (68.85), H, 9.72 (9.43), N, 3.97 (4.23). μ_{eff} (C_6D_6, 21 °C) = 5.5(3) μ_B. ^{1}H NMR (C_6D_6, 21 °C): 115 (1H, α-CH), 70.7 (9H, $(CH_3)_3$Si), 43.8 (18H, $(CH_3)_3$C−L), −26.1 (14H, ^{i}Pr−CH_3, *m*-CH), −106.0 (4H, ^{i}Pr−CH), −120.0 (12H, *p*-CH, ^{i}Pr−CH_3, *p*-CH).

Spectroscopic Observation of L^{tBu}Fe(μ-S)FeL^{tBu}. When **2** and HMDS are reacted in equimolar amounts, this sulfide complex was formed along with **4** in a 1:1 ratio. The ^{1}H NMR spectrum is very similar to that of the related sulfide complex L^{Me}Fe(μ-S)FeL^{Me}.[16] ^{1}H NMR (C_6D_6, 21 °C): 23.9 (1H, α-CH), 12.4 (18H, $(CH_3)_3$C−L), 6.2 (4H, *m*-CH), −2.3 (12H, ^{i}Pr−CH_3), −7.0 (4H, ^{i}Pr−CH), 18.5 (2H, *p*-CH), 19.0 (12H, ^{i}Pr−CH_3).

Reaction of [L^{Me}Fe(μ-F)]$_2$ ($\mathbf{1_2}$) with Hexamethyldisilathiane. The reaction of $\mathbf{1_2}$ (9.8 mg, 10 μmol) and HMDS (4.3 μL, 20 μmol) proceeded cleanly in C_6D_6 at 60 °C for 4 h to give L^{Me}Fe(μ-S)FeL^{Me} (100% by ^{1}H NMR).[16]

L^{tBu}FeCCSiMe_3 (5). Prepared in a similar way to **3** from bis(trimethylsilyl)acetylene (140 μL, 0.62 mmol) and **2** (180 mg, 0.31 mmol): 124 mg, 61%. Anal. Found (calcd): C, 73.17 (73.36), H, 9.32 (9.54), N, 4.36 (4.28). μ_{eff} (C_6D_6, 21 °C) = 5.8(3) μ_B. ^{1}H NMR (C_6D_6, 21 °C): 112 (1H, α-CH), 57.4 (9H, $(CH_3)_3$Si), 43.1 (18H, $(CH_3)_3$C−L), −27.7 (12H, ^{i}Pr−CH_3), −32.5 (2H, *m*-CH), −116 (18H, *p*-CH, ^{i}Pr−CH_3, ^{i}Pr−CH). IR (KBr pellet, cm^{-1}): 2092 (νC≡C).

[L^{Me}Fe(μ-H)]$_2$ ($\mathbf{6_2}$). Prepared in a similar way to **3** and **4**, from triethylsilane (61 μL, 0.38 mmol) and $\mathbf{1_2}$ (188 mg, 0.19 mmol): 160 mg, 89%. Anal. Found (calcd): C, 73.14 (73.41), H, 8.39 (8.92), N, 5.98 (5.90). μ_{eff} (C_6D_6, 21 °C) = 4.0(3) μ_B. ^{1}H NMR (C_6D_6, 21 °C): 13.2 (12H, ^{i}Pr−CH_3), 3.2 (2H, *p*-CH), 1.1 (4H, *m*-CH), −24.6 (18H, ^{i}Pr−CH_3, CH_3−L), −57.6 (4H, ^{i}Pr−CH). Virtually identical ^{1}H resonances and chemical shifts were observed at room temperature in THF-d_8, indicating that in contrast to the L^{tBu} analogue $\mathbf{7_2}$,[17] $\mathbf{6_2}$ does not dissociate into a monomer in the absence of strong donor ligands (e.g., pyridine).

Reaction of L^{tBu}FeF (2) with Et_3SiH. A J. Young NMR tube was loaded with **2** (10 mg, 17 μmol), Et_3SiH (2.8 μL, 17 μmol), and C_6D_6 (0.4 mL). The tube was sealed and heated to 45 °C for 12 h. Complete conversion to $\mathbf{7_2}$ (^{1}H NMR) and Et_3SiF (^{19}F NMR, α,α,α-trifluorotoluene used as internal standard, see below) was observed.

HDF of Fluoroarenes. A J. Young NMR tube was loaded with a solution of substrate ([ArF] = 0.11 M), a trisubstituted silane ([R_3SiH] = 0.11 M), and one of $\mathbf{1_2}$, $\mathbf{6_2}$, $\mathbf{7_2}$ (0.01 M), or **2** (0.02 M). The tube was heated to the specified temperature in an oil bath, and NMR spectra (^{19}F, ^{1}H) were recorded periodically. A capillary containing a solution of α,α,α-trifluorotoluene was used as an internal standard for chemical shift and integration purposes. HDF products were identified by a combination of ^{19}F NMR and GC-MS data. In all cases, fluorotriethylsilane was observed by ^{19}F NMR (−176.7 ppm) and by GC-MS analysis of the reaction mixture (F−$SiEt_3$, *m*/*z* = 134).

Kinetics of Perfluoroarene HDF. The above procedure was repeated with octafluorotoluene while varying the initial concentrations of reactants (one at a time).[37] The sample was placed on a previously equilibrated and temperature-calibrated[53] NMR probe, and ^{19}F spectra were recorded periodically. Monitoring was continued up to 10−20 mol % substrate conversions. When triethylsilane-*d* was used, deuterium incorporation into the HDF product was observed by GC-MS (DC_6F_4-CF_3 *m*/*z* = 219).

Radical Scavenger Experiments. The octafluoroarene HDF was repeated as described above and in parallel with and without one of the radical traps dihydroanthracene (0.047 M, 0.43 equiv) or triphenylmethane (0.044 M, 0.40 equiv).

HDF of Fluoroolefins. The above procedure was repeated, but the gaseous olefinic substrate (hexafluoropropene or 3,3,3-trifluoropropene)

(53) (a) Ammann, C.; Meier, P.; Merbach, A. E. *J. Magn. Reson.* **1982**, *46*, 319−321. (b) Kaplan, M. L.; Bovey, F. A.; Cheng, H. N. *Anal. Chem.* **1975**, *47*, 1703−1705.

Table 6. Details of X-ray Crystal Structures

	$[L^{Me}Fe(\mu\text{-}F)]_2$ (**1_2**)	$L^{tBu}FeF$ (**2**)	$L^{tBu}FeF$(4-^{t}Bu-py) (**2·^{t}Bupy**)	$L^{tBu}FeSSiMe_3$ (**4**)	$L^{tBu}FeCCSiMe_3$ (**5**)
empirical formula	$C_{58}H_{82}F_2Fe_2N_4$	$C_{35}H_{53}FFeN_2$	$C_{44}H_{66}FFeN_3$	$C_{38}H_{62}FeN_2SSi$	$C_{40}H_{62}FeN_2Si$
fw	984.98	576.64	711.85	662.90	654.86
cryst syst	monoclinic	monoclinic	monoclinic	monoclinic	monoclinic
space group	*C*2/*c*	*C*2/*c*	$P2_1/c$	$P2_1/n$	$P2_1/c$
a (Å)	15.2552(10)	23.480(3)	13.9028(6)	15.4030(8)	16.941(2)
b (Å)	16.7611(11)	8.5555(11)	20.4954(9)	26.3684(15)	12.5476(16)
c (Å)	21.8794(14)	17.105(2)	18.8040(6)	19.7988(11)	19.408(3)
β (deg)	91.1460(10)	108.491(3)	128.169(2)	97.3040(10)	90.781(2)
V (Å^3)	5593.3(6)	3258.7(7)	4212.5(3)	7976.1(8)	4125.3(9)
Z	4	4	4	8	4
ρ (g/cm^3)	1.170	1.175	1.122	1.104	1.054
μ (mm^{-1})	0.563	0.493	0.394	0.486	0.421
R1, wR2 ($I > 2\sigma(I)$)	0.0543, 0.1057	0.0409, 0.0886	0.0523, 0.1150	0.0479, 0.0779	0.0453, 0.0953
GOF	1.076	1.030	1.016	0.899	1.044

	$L^{Me}FeF$(4-^{t}Bu-py) (**1·^{t}Bupy**)	$L^{Me}FeF$(4-CF_3-py)·(THF) (**1·CF_3py·**THF)	$L^{tBu}FeF(NCCH_3)$·(CH_3CN) (**2·ACN·**ACN)	$L^{tBu}FeOEt_2(\eta^1\text{-}BF_4)$ (**3**)	$[L^{Me}Fe(\mu\text{-}H)]_2$·($OEt_2$) (**$6_2$·**$OEt_2$)
empirical formula	$C_{38}H_{54}FFeN_3$	$(C_{38}H_{51}F_4FeN_3)\cdot(C_4H_8O)$	$C_{39}H_{59}FFeN$	$C_{39}H_{63}BF_4FeN_2O$	$(C_{58}H_{84}Fe_2N_4)\cdot(C_4H_{10}O)$
fw	627.69	753.77	658.75	718.57	1023.11
cryst syst	triclinic	triclinic	triclinic	triclinic	monoclinic
space group	$P\bar{1}$	$P\bar{1}$	$P\bar{1}$	$P\bar{1}$	$P2_1/c$
a (Å)	8.6321(10)	8.9028(8)	9.8640(9)	10.0195(11)	11.5959(15)
b (Å)	12.4465(14)	12.6570(11)	12.2956(11)	12.4908(13)	18.315(2)
c (Å)	18.430(2)	18.2746(15)	17.9941(16)	18.648(2)	28.590(4)
α (deg)	92.217(2)	93.3230(10)	96.695(2)	107.879(2)	90
β (deg)	91.025(2)	101.575(2)	97.672(2)	103.667(2)	98.870(2)
γ (deg)	99.486(2)	94.635(2)	112.544(2)	91.076(2)	90
V (Å^3)	1951.0(4)	2004.9(3)	1963.7(3)	7976.1(8)	5999.4(13)
Z	2	2	2	2	4
ρ (g/cm^3)	1.068	1.249	1.114	1.111	1.133
μ (mm^{-1})	0.417	0.430	0.418	0.397	0.524
R1, wR2 ($I > 2\sigma(I)$)	0.0956, 0.2932	0.0860, 0.2304	0.0944, 0.1910	0.0399, 0.1157	0.0791, 0.1954
GOF	1.281	1.039	1.390	1.122	1.048

was condensed from a calibrated volume bulb into a resealable NMR tube containing a THF-d_8 solution of **1_2** (0.01 M) and triethylsilane (0.11 M). The individual HDF products, 1,2,3,3,3-pentafluoropropene ($CHF{=}CFCH_3$, both *E* and *Z* isomers),[54] 1,1,3,3,3-pentafluoropropene ($CF_2{=}CHCF_3$),[55] or 1,1-difluoropropene ($CF_2{=}CHCH_3$),[5b,56] were identified by ^{19}F NMR by comparison to the reported data on chemical shifts and coupling constants for each of these compounds, as well as by GC-MS (m/z = 132). Relative concentrations of reactant and products were obtained from integration of ^{19}F resonances, assuming that all gases had similar solubility. During the HDF of α,α,α-trifluoropropene, the only species observed by NMR was the previously reported alkyl complex $L^{Me}FeCH_2CH_2CF_3$.[18a] ^{1}H NMR (THF-d_8, 21 °C): 159.0 (2H, *p*-CH), 10.7 (4H, *m*-CH), 0.5 (12H, ^{i}Pr−CH_3), −18.4 (1H, α-CH−L), −30.7 (12H, ^{i}Pr−CH_3), −45.1 (4H, ^{i}Pr−CH), −45.7 (6H, CH_3−L). ^{19}F NMR (THF-d_8, 21 °C): 46 ppm (3H, CF_3 terminus). A similarly distinctive paramagnetically broadened signal at 53 ppm (presumably attributable to $L^{Me}FeCF_2CF_2CF_3$) was observed by ^{19}F NMR during the HDF of hexafluoropropene. Neither fluoride nor hydride species were observed by NMR during catalysis.

Oxidation of Hydride Complexes. Electrochemical Study. Cyclic voltammetry measurements on $[L^{Me}FeH]_2$ **6_2** and $[L^{tBu}FeH]_2$ **7_2** were carried out under an inert atmosphere (≤1 ppm O_2) with a Cypress Systems Potentiostat/Electroanalytical System CS-1200 inside an argon drybox. A glassy graphite electrode was used as the working electrode, and two silver wires were used as auxiliary and reference electrodes. The CV experiments were performed in THF at room temperature with 0.2 M NBu_4OTf supporting electrolyte (Aldrich, 99%) and 0.003 M analyte. The scan rate in all experiments was 0.1 V/s. Both hydride complexes showed an irreversible oxidation at −0.4 V vs the Ag electrode (ca. −0.6 V vs ferrocene (Fc); ferrocene could not be used directly as an internal reference because it showed noninnocent behavior during the electrochemical experiments). **Chemical study.** To substantiate the results of the electrochemical experiments, the hydride complexes were exposed to two chemical oxidants of varying strength in THF-d_8 and the fate of the reaction followed by ^{1}H NMR. A stoichiometric amount of either $Cp_2Fe^+B(ArF)^-$ ($E°_{rel}$ = 0 V; $B(ArF)^-$ = tetrakis(3,5-bis(trifluoromethyl)phenyl)borate)[57] or even the weaker oxidant $Cp^*_2Fe^+B(ArF)^-$ ($E°_{rel}$ = −0.59 V vs Fc)[57] instantaneously reacts with the hydride complexes. Formation of Cp_2Fe (4.05 ppm) and Cp^*_2Fe (1.42 ppm) was observed by ^{1}H NMR spectroscopy, along with paramagnetic products that were not further characterized.

X-ray Structures. Crystalline samples were grown in the glovebox from pentane or ether solutions at −38 °C. Each sample was rapidly mounted under Paratone-8277 onto a glass fiber and immediately placed in a cold nitrogen stream at −80 °C on the X-ray diffractometer. X-ray intensity data were collected on a standard Bruker-axs SMART CCD area detector system equipped with a normal focus molybdenum-target X-ray tube operated at 2.0 kW (50 kV, 40 mA). A total of 1121 frames (for **1_2**, **2·ACN**, **4**, and **6_2**) or 2424 frames (for **2**, **3**, **5**, **1·^{t}Bupy**, **1·CF_3py**, and **2·^{t}Bupy**) of data were collected using a narrow frame method with scan widths of 0.3° in ω. Frames were integrated to a maximum 2θ angle of 56.6° with SAINT. The final unit cell parameters (at −80 °C) were determined from the least-squares refinement of three-dimensional centroids of >4000 reflections for each crystal. Data were

(54) (a) Koroniak, H.; Palmer, K. W.; Dolbier, W. R.; Zhang, H. *Magn. Reson. Chem.* **1993**, *31*, 748−751. (b) Burton, D. J.; Spawn, T. W.; Heinze, P. L.; Bailey, A. R.; Shin-Ya, S. *J. Fluorine Chem.* **1989**, *44*, 167−174.
(55) Fields, R.; Germain, M. M.; Haszeldine, R. N.; Wiggans, P. W. *J. Chem. Soc. (A)* **1970**, 1961−1974.
(56) Shaler, T. A.; Morton, T. H. *J. Am. Chem. Soc.* **1991**, *113*, 6771−6779.
(57) Connelly, N. G.; Geiger, W. E. *Chem. Rev.* **1996**, *96*, 877−910.

corrected for absorption with the SADABS[58] program. The space groups were assigned using XPREP, and the structures were solved by direct methods and refined employing full-matrix least-squares on F^2 (Bruker-axs, SHELXTL-NT,[59] version 5.10). All non-H atoms were refined with anisotropic thermal parameters. Iron-bound hydrogen atoms in $\mathbf{6_2}$ were located in the electron density map and refined with isotropic thermal parameters. All other hydrogen atoms were included in idealized positions. The structures refined to goodness of fit values and final residuals found in Table 6.

(58) The SADABS program is based on the method of Blessing; see Blessing, R. H. *Acta Crystallogr. A* **1995**, *51*, 33−38.
(59) *SHELXTL NT*: Structure Analysis Program, version 5.10; Bruker-AXS: Madison, WI, 1995.

Acknowledgment. Funding for this work was provided by the National Science Foundation (CHE-0112658), the Petroleum Research Fund (38275-G to P.L.H.), the A. P. Sloan Foundation (Research Fellowship to P.L.H.), and the University of Rochester (Hooker and Messersmith fellowships to J.V.). We are indebted to Bill Jones, Brad Kraft, Joe Dinnocenzo, and an anonymous reviewer for helpful comments, and to Karin Ruhlandt for the use of an X-ray diffractometer.

Supporting Information Available: Additional spectroscopic and crystallographic data. This material is available free of charge via the Internet at http://pubs.acs.org.

JA042672L